J. Fluid Mech. (1994), *vol.* 259, *pp.* 47–78

Compressibility effects on the structure of supersonic mixing layers: experimental results

By S. BARRE, C. QUINE AND J. P. DUSSAUGE

Institut de Mécanique de Marseille, Institut de Mécanique Statistique de la Turbulence, U.M. CNRS-Université Aix-Marseille II no 380033, 12 avenue de Général Leclerc, 13003 Marseille, France

(Received 27 January 1992 and in revised form 8 July 1993)

An experiment in a supersonic mixing layer at convective Mach number $M_c = 0.62$ was performed to study the evolution of a flow from a turbulent boundary layer to a fully developed mixing layer. Turbulence measurements were taken and are interpreted with a diffusion model, which is well adapted to these flows. These measurements show that the level of turbulent friction varies with M_c proportionally to the spread rate. Our measurements appear to be consistent with the spreading rate of the layer and suggest that compressibility does not significantly alter the diffusion scheme at $M_c = 0.62$. This is also confirmed by a review of the existing data. Moreover, in the present flow, the anisotropy of the turbulent stresses seems to be affected by compressibility. The evolution of the radiated noise shows an increase corresponding to the developed part of the layer. Quantitative assessments of compressibility effects on turbulent quantities are given and are related to modifications in the structure of the flow.

1. Introduction

In high-speed mixing layers, the structure of turbulence is strongly affected by compressibility. For example, the spreading rate of the mixing layer decreases sharply with the Mach number (Sirieix & Solignac 1968; Brown & Roshko 1974) as compared to incompressible mixing layers at the same free-stream velocity and density ratios. Compressibility inhibits the entrainment of mass and, more generally, turbulent diffusion.

A qualitative explanation of this phenomenon may be inferred from an analysis of the linear stability of a two-dimensional vortex sheet (Pai 1954; Miles 1958). This explanation has been recently popularized by many authors (Norman & Winkler 1985; Papamoschou & Roshko 1988); it considers the convection velocity (or more precisely the convective Mach number defined below) of the eddies in the mixing layer. If this velocity is supersonic with respect to the external flow (or in a equivalent way if the convective Mach number of the eddies is supersonic), the pressure perturbations induced by the eddies are Mach waves, and propagate very far into the outer flow. This peculiarity of high-speed flows may greatly alter the turbulent field. For example, some particular features may become important, such as eddy shocklets produced by the large eddies, or sonic disturbances as observed in jets by Oertel (1979). This simplified picture, which leads to significant modification of the turbulence models used for compressible flows (Zeman 1990; Sarkar *et al.* 1989) does not describe all the modifications due to compressibility. Stability analysis, numerical simulations (Sandham & Reynolds 1989) and flow visualizations (Clemens & Mungal 1990; Bonnet & Debisschop 1993) show that three-dimensional effects are also more important in

compressible flows. The key point of these analyses is, of course, to know the convection speed of the turbulent structure. Bogdanoff (1983) and Papamoschou (1986) have used the convective Mach number M_c to quantify this compressibility effect. This Mach number is based on the velocity difference between the convection of the eddies and the external flow. It is evaluated in two-dimensional flows by the approximation of an isentropic compression in the vicinity of the stagnation point between any two vortices. This yields a first means of determining the convective Mach number. However, some experiments suggest that the isentropic approximation is not obeyed for $M_c > 0.6$. The reasons for this departure are not yet completely known, although some suggestions have been proposed to explain the unexpected convection velocity measured in some flows. For example, there may exist eddy shocklets which lead to non-isentropic compression (Papamoschou 1989; Dimotakis 1991). From the experimental observations (Papamoschou 1989; Hall 1991; McIntyre & Settles 1991) it seems that for large values of the isentropic convective Mach number, the eddies move practically with the speed of one of the external flows.

The goal of the present work is to help clarify the effect of compressibility on mixing layers through an experimental study of a mixing layer downstream of a splitter-plate trailing edge. The external Mach numbers of the initial boundary layers ($M_1 = 1.8$ and $M_2 = 0.3$) are such that, according to Morkovin's hypothesis, only weak effects of Mach number should be found in the structure of turbulence of these initial boundary layers. It will be seen from experiments that the Mach number of fluctuations is about 0.3 in the mixing layer. Therefore this experiment describes some developments of compressibility effects as the mixing layer approaches its asymptotic state.

In the first part of this paper, the influence of compressibility on the turbulent fluxes is characterized by the use of a phenomenological analysis. This analysis is developed mainly to classify the experimental results. The experiment will then be described and followed by a presentation of the results for the mean and turbulent quantities, including measurements of radiated noise in the outer flow. Lastly, the results will be interpreted and discussed.

2. Phenomenological background

A shear layer is considered in which large eddies are formed. The velocity difference between the two external flows is $\Delta U = U_1 - U_2$. The eddies are assumed to be transported with a convection velocity U_c and to diffuse momentum with an effective (turbulent) diffusivity coefficient μ_t. They have a characteristic lengthscale δ, where δ is some measure of the size of these eddies. A temporal analysis is proposed where it is supposed that the relevant parameter is the diffusion time in a convected frame of reference. This timescale, for supersonic flows with variable density, is assumed to have the form $t = t(\delta, \mu_t, \rho, M)$, where ρ is the density and M is a Mach number related to U_c. From dimensional arguments, a form for this timescale can be

$$t = k_1(s, M)\,\delta^2/\nu_t,$$

where $s = (\rho_2/\rho_1)$ is the density ratio between the two external flows and $\nu_t = \mu_t/\rho$ with ρ chosen in the part of the flow where μ_t is significant. It is supposed that ν_t is nearly constant across the flow. The use of kinematic variable ν_t implies that k_1 is also a function of the density ratio s and not only of the Mach number. This expression suggests that in low-speed flows ($M \to 0$) the diffusion time may depend on density variations. It implicitly assumes that the flow can be characterized only by s; therefore

it is expected that the results will hold mainly for flows in which the density profiles are practically self-similar.

In the same way, the Mach-number dependence of k_1 implies that vortices may need a different time to grow if they produce shocklets, or if compressibility causes a change in their shape, for example by increasing their three-dimensionality.

It will be assumed here that k_1 is independent of the Reynolds number. This assumption seems to be acceptable if the Reynolds number is large enough that the flow is fully turbulent. For large Reynolds numbers (for example if there are no effects of transition), increasing this parameter will correspond to the creation of small-scale structures. Such an effect can be observed in probability density functions or in energy spectra: the dissipative range becomes different from the energetic one, the Kolmogorov scale becomes smaller and the spectrum can contain very large-wavenumber components. However, this phenomenon involves small-scale fluctuations of lower and lower amplitude, so that, if the Reynolds number is large enough, their contribution to the energy or to the Reynolds stress is supposed to be practically negligible and, consequently, k_1 does not depend on the Reynolds number.

The order of magnitude of the eddy diffusivity is now considered. It is assumed that ν_t is constant across the flow. This corresponds to the traditional model first introduced by Prandtl at the beginning of the century, and used by Görtler (quoted by Schlichting 1964, pp. 689–690) to calculate the mean velocity profiles in free shear flows. A rather good approximation of their shape was then obtained. Second-order closures for these compressible flows can be found in Sarkar *et al.* (1989) and Zeman (1992) who included hypotheses to account for compressible turbulence. These models give a reasonable rate of spread for the supersonic mixing layer. The latter reference suggests that the eddy viscosity is practically constant in the main part of the flow, and it seems convenient to use this assumption for dimensional analysis. So, ν_t can be given by

$$\nu_t = \frac{u_\tau^2}{(\partial u/\partial y)_{\max}},$$

where $u_\tau^2 = \tau/\rho$; τ is the maximum shear stress level in the layer and ρ is the local mean density. The maximum velocity gradient $(\partial u/\partial y)_{max}$ is estimated as

$$(\partial u/\partial y)_{max} = k_2(\Delta U/\delta).$$

From experimental evidence (Samimy & Elliott 1990; Dutton *et al.* 1990; Ikawa & Kubota 1975), the shape of the velocity profile is not sensitive to the Mach number. A more detailed analysis of necessary conditions for similarity has been proposed by Zeman (1992). It shows that compressibility introduces some difficulties in reaching a similar state, but the computations indicate that the shape of the velocity profile is not significantly affected by this effect in a wide range of convective Mach numbers up to 4. Accordingly, it will be supposed that the shape of the velocity profile does not depend on the Mach number.

Then k_2 is assumed constant, that is $\partial k_2/\partial M = 0$, and finally

$$t = k_1 k_2 \delta(\Delta U/u_\tau^2).$$

To transform the time dependence into a space variation we must define a convection velocity U_c: $x = U_c t$. U_c is taken as a function of s and M_c but does not have to be more precisely specified yet. In the simple representation currently used for a given flow, there is a single convection velocity, such that the eddies have a constant shape

and are considered as 'frozen patterns'. The linear spreading of the mixing layer is deduced:

$$\left(\frac{\mathrm{d}\delta}{\mathrm{d}x}\right)_t = \frac{1}{K(s, M_c)} \frac{u_\tau^2}{(\Delta U\, U_c)}. \tag{1a}$$

The quantity $K(s, M_c) = k_1 k_2 = (tu_\tau^2)/(\delta \Delta U)$ which can be interpreted like a 'normalized diffusion time' depends on Mach number and density ratio through k_1. The function $K(s, M_c)$ has to be determined from experiment. If U_c is known, Mach numbers with respect to the external flows can be defined as normal: $M_{c1} = (U_1 - U_c)/a_1$, $M_{c2} = (U_c - U_2)/a_2$. When the eddies produce no shocklets, the convective Mach number can be defined as $M_c = M_{c1} = M_{c2} = \Delta U/(a_1 + a_2)$. It is assumed, as proposed by Papamoschou (1989), that M_c is a pertinent parameter to classify compressibility effects, even when $M_{c1} \neq M_{c2}$. Equation (1*a*) has the same form as the estimate used by Brown & Roshko (1974) from dimensional arguments based on the momentum equation. In Brown & Roshko's derivation some unspecified velocity scale U is found instead of U_c. U is of the order of the average velocity, but is not defined as the local mean velocity.

Relation (1*a*) corresponds to the spreading rate of a temporal mixing layer. The growth rate of the corresponding spatial mixing layer may be different because of the unsymmetric entrainment ratio of spatially evolving mixing layers as discussed by Dimotakis (1986). This author has proposed a model to represent the entrainment rate in mixing layers with variable density. It reproduces well the growth rate variation due to density ratio changes in subsonic mixing layers. A correction function f_d is deduced to obtain the spatial growth rate from the temporal one for subsonic mixing layers, and the expression for the spatial growth rate is obtained:

$$\left(\frac{\mathrm{d}\delta}{\mathrm{d}x}\right)_{sp} = \left(\frac{\mathrm{d}\delta}{\mathrm{d}x}\right)_t f_d(s, M_c) = \frac{f_d(s, M_c)}{K(s, M_c)} \frac{u_\tau^2}{\Delta U\, U_c}, \tag{1b}$$

where $f_d(s, M_c)$ is a temporal-to-spatial correction function which depends on density ratio and convective Mach number. It is supposed here that s and M_c are separable variables, such that the influence of s is the same for $M_c \to 0$ and for the high-speed case. For the range of density ratios corresponding to the compilation of data studied later in this paper ($0.38 \leqslant s \leqslant 1.56$) (see §4.2), Dimotakis's correction function f_d gives very weak corrections (maximum 5%) to the growth rate value. This is rather low and seems negligible compared to the important decrease of the growth rate due to compressibility effects.

Another possible way to express the spreading rate is the usual empirical expression proposed by Papamoschou (1986):

$$\left(\frac{\mathrm{d}\delta}{\mathrm{d}x}\right)_{sp} = 0.5 \left(\frac{\mathrm{d}\delta}{\mathrm{d}x}\right)_{ref} \frac{\Delta U}{U_c} \phi(M_c) f_d(s, M_c), \tag{2}$$

where $(\mathrm{d}\delta/\mathrm{d}x)_{ref}$ is the spreading rate of the subsonic shear layer with $U_0 = 0$ and constant density. $\phi(M_c)$ is a function of the convective Mach number. Note that Papamoschou (1986) assumes that $f_d \approx 1$, but he points out that such a function should be introduced to compare the results of spatial and temporal theories.

In addition, following Bogdanoff (1983) and Papamoschou & Roshko (1988), it will be assumed that the convective Mach number M_c is the correct parameter to quantify compressibility effects, even if the determination of U_c is questionable (Papamoschou 1989; Dimotakis 1991).

Equations (1*b*) and (2) combine to given an expression for $K(s, M_c)$:

$$K(s, M_c) = \frac{u_\tau^2/(\Delta U)^2}{\frac{1}{2}(\mathrm{d}\delta/\mathrm{d}x)_{ref}\,\phi(M_c)} = \frac{u_\tau^2/(\Delta U)^2}{(\mathrm{d}\delta/\mathrm{d}x)(U_c/\Delta U)}, \tag{3}$$

which can be rewritten to give an expression for the turbulent friction as a function of the spreading rate:

$$(\overline{-u'v'}_{max}/(\Delta U)^2) = \tfrac{1}{2}K(s, M_c)(\mathrm{d}\delta/\mathrm{d}x)_{ref}\,\phi(M_c). \tag{4}$$

The normalized diffusion time $K(s, M_c)$, which is a function of s and M_c, has to be determined from experiments. If the influence of these parameters can be separated, the influence of the density ratio can be deduced from low-speed studies, while supersonic experiments will give us the Mach-number contribution.

Concerning the density ratio influence on K, unfortunately few data are available in subsonic flows (Fiedler, Lummer & Nottmeyer 1990 and Nottmeyer 1990 for mixing layers, Panchapakesan & Lumley 1993*a*, *b* and Djeridane *et al.* 1993 for jets). These results are partial and cover only a limited range of density ratios, so that they are of limited use for application to high-speed flows. An attempt has been made to use these data, but their scarcity and scatter made the determination of the density ratio influence on $K(s, M_c)$ inaccurate and it was preferred not to use them in the present work.

However, it was felt that relations (1)–(4) could be used as useful guides to interpret data in supersonic mixing layers and suggest some links between turbulent friction and rate of spread.

If the dependence of u_τ on M_c is known, other results can be deduced for some turbulent quantities. For example, the maximum level of turbulence production may be estimated as

$$P = u_\tau^2(\Delta U/\delta) = P_{ref}\,K(s, M_c)\,\phi(M_c).$$

P_{ref} is the rate of turbulence production in a subsonic shear layer with the same velocity gradient. Then, if K is a weak function of M_c for a given s, turbulence production decreases with M_c as the spreading rate. A last illustration of the influence of M_c can be given by the length of dissipation, as used by Bradshaw & Ferriss (1971). A rough but significant approximation consists in assuming that production and dissipation rates are practically equal, $P \approx \epsilon$. The dissipation length l is defined by $\epsilon = u_\tau^3/l$. The dependence of l/δ on M_c is straightforward:

$$l/\delta = u_\tau/\Delta U = (l/\delta)_{ref}[K(s, M_c)\,\phi(M_c)]^{\frac{1}{2}}.$$

Again, if K is a weak function of s, this relation shows that a decrease of ϵ, through $\phi(M_c)$, is accompanied also by a decrease of l/δ and suggests that smaller scales are involved in dissipation in compressible shear flows.

3. Experimental results

3.1. *Experimental set-up*

The experiments were performed in the supersonic wind tunnel at IMST. This is a closed-circuit, continuously operating, supersonic wind tunnel. The stagnation conditions of the flow were kept practically constant for several hours. The test section was 15×14 cm^2 and the level of turbulence in the nozzle was very low, typically 0.2%. The mixing layer was obtained, as shown in figure 1(*a*), by mixing two independently controlled streams separated by a splitter plate. The supersonic flow (flow 1) is the IMST supersonic wind tunnel flow. The stagnation pressure of this flow is 0.6

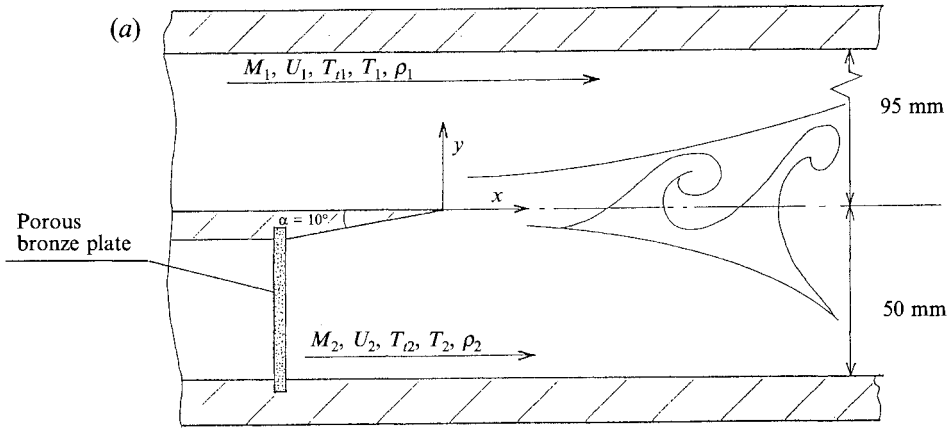

(b)

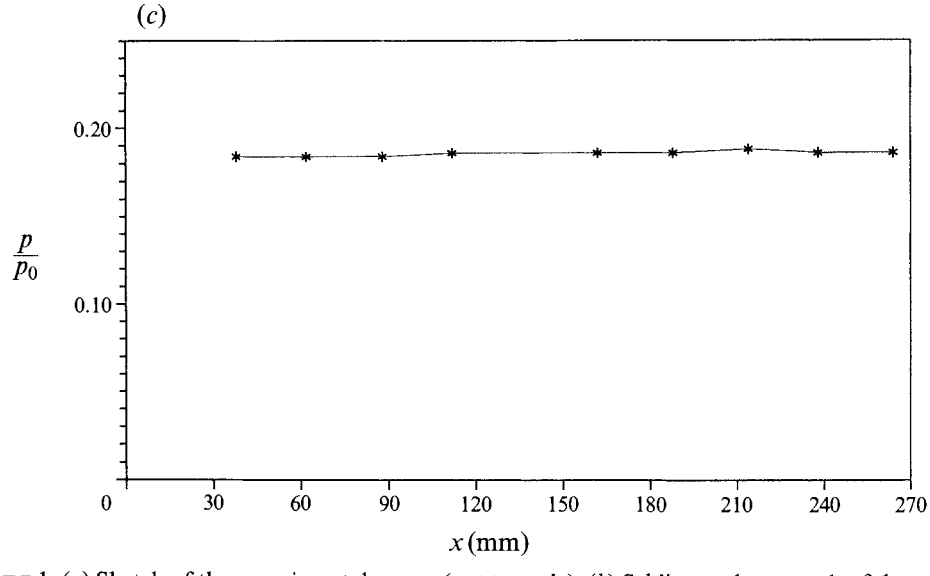

FIGURE 1. (*a*) Sketch of the experimental set-up (not to scale). (*b*) Schlieren photograph of the mixing layer. The right side of the view is located at $x = 50$ mm and the left side at $x = 200$ mm. (*c*) Streamwise evolution of the low-speed sidewall pressure along the test section (pressure related to stagnation condition).

	M	$U(\mathrm{m\ s^{-1}})$	$T_t(\mathrm{K})$	$T(\mathrm{K})$	$\rho(\mathrm{Kg\ m^{-3}})$
Flow 1	1.79	481	296	180	0.208
Flow 2	0.30	101	291	286	0.130

TABLE 1. Main characteristics of the two flow fields

atmospheres. It is kept constant by a regulated vacuum system. The other flow (flow 2) is subsonic. Because of the particular shape of the test section, there was no room to design a classical complete settling chamber for the low-speed flow, and so the latter was homogenized using a screen of porous bronze. This screen acted also to damp turbulence. Characteristics of the incoming flows are given in §3.3.3. From these results it appears that the developed part of the mixing layer does not depend much on the particular conditions at the trailing edge (see §4.1). The mass flux of the subsonic stream was adjusted to produce an isobaric mixing layer. The Mach number M_1 in the outer flow was 1.8, and $M_2 = 0.3$ in the inner flow. The stagnation temperature T_t was approximately atmospheric. The convective Mach number determined from isentropic relations was 0.62. Further details are given by Quine (1990). It should be noted that the initial boundary layer on the high-speed side was turbulent and fully developed. Measurements were taken over a distance equivalent to about 25 initial boundary-layer thicknesses, or 320 times the momentum thickness. A spark schlieren photograph of the flow is shown in figure 1(*b*). The exposure time is about 1 μs. The trailing edge of the plate cannot be seen on this picture. The right end of the layer is located at $x = 50$ mm; the downstream sections where a pressure probe is visible correspond to $x = 200$ mm. Large-scale structures appear very clearly in the mixing layer. In the upper right part of the picture, Mach waves originating at the trailing edge can be seen. They are reflected by the upper wall, but they intercept the mixing layer far downstream from the last measurement section ($x = 200$ mm). Figure 1(*c*) gives the distribution of static pressure along the lower wall of the test section. Note that no significant pressure gradient is applied to the layer.

3.2. *Mean fields*

Mean quantities were measured using classical methods: a flattened Pitot probe (height of the probe: 0.3 mm) for total pressure, a bevelled static probe (Type ONERA 20K10) for static pressure and a vented thermocouple for total temperature. Velocity, temperature and density were deduced from the direct measurements by the usual methods (Liepmann & Roshko 1962).

The main characteristics of the flow are summarized in table 1. These characteristics give $r = U_2/U_1 = 0.21$; $s = \rho_2/\rho_1 = 0.625$ and $M_c = 0.62$.

Figures 2(*a*) and 2(*b*) show profiles of the mean velocity U at various locations. The origin of the frame of reference is located at the trailing edge of the flat plate, as indicated in figure 1(*a*). The shapes of the profiles indicate the evolution from a boundary layer ($x = 1$ mm), to a mixing layer ($x > 160$ mm). Note that the wake rapidly disappears within the first sections because ΔU is rather large.

Quine (1990) has shown that the boundary layer on the high-velocity side was turbulent and in equilibrium. Figure 3 shows the Van Driest transformed velocity profile in semi-logarithmic form. In applying the Van Driest transformation,

$$V = \int_0^u (\rho/\rho_w)^{\frac{1}{2}}\,\mathrm{d}u,$$

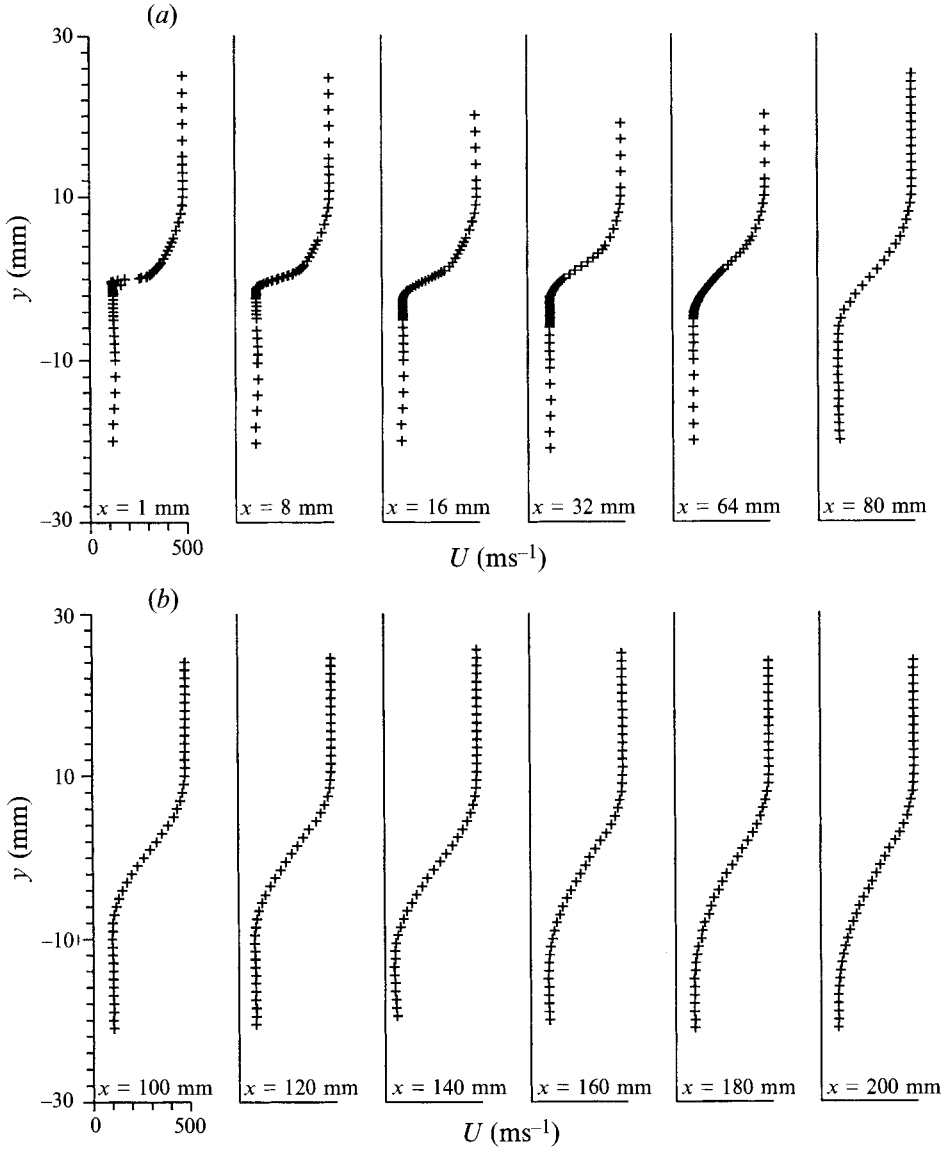

FIGURE 2. Mean velocity profiles.

the experimental values of ρ were used. The friction velocity u_τ was calculated from the semi-empirical theory of Fernholz (1971). Figure 3 shows a satisfactory agreement with the law of the wall. The boundary layer developing on the low velocity side of the plate was very thin, with a thickness of less than 1 mm. This was probably laminar. The influence of the nature of this layer will be checked and will be discussed in §4. Table 2 summarizes the main characteristics of the initial turbulent boundary layer. M_e is the external Mach number.

As was mentioned in the previous section, mixing layers are very sensitive to initial and boundary conditions. This was pointed out by Bradshaw (1966) for subsonic flows, and the review by Dimotakis (1991), including variable-density cases, confirms that macroscopic quantities like the spreading rate depend critically on the method used to produce the flow, such that huge scatter is found on these quantities, even at low speed.

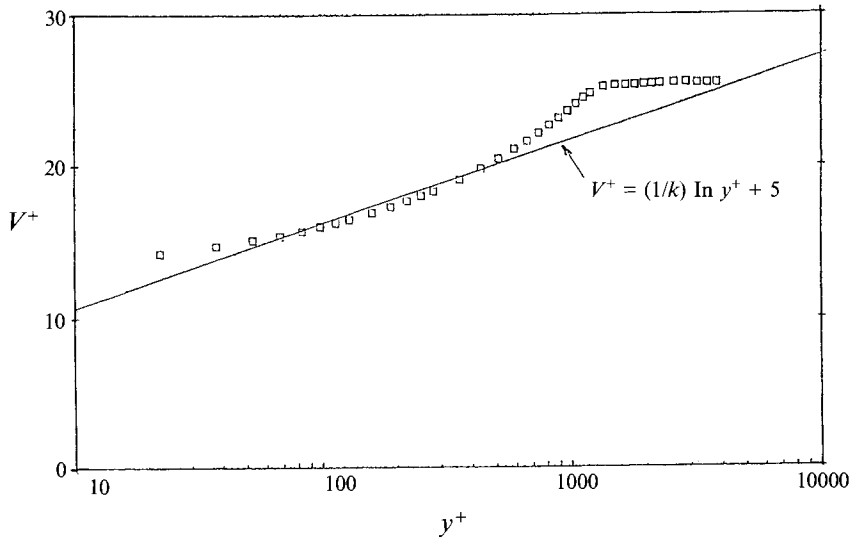

FIGURE 3. Van Driest transformed velocity profiles in the initial boundary layer ($x = -5$ mm).

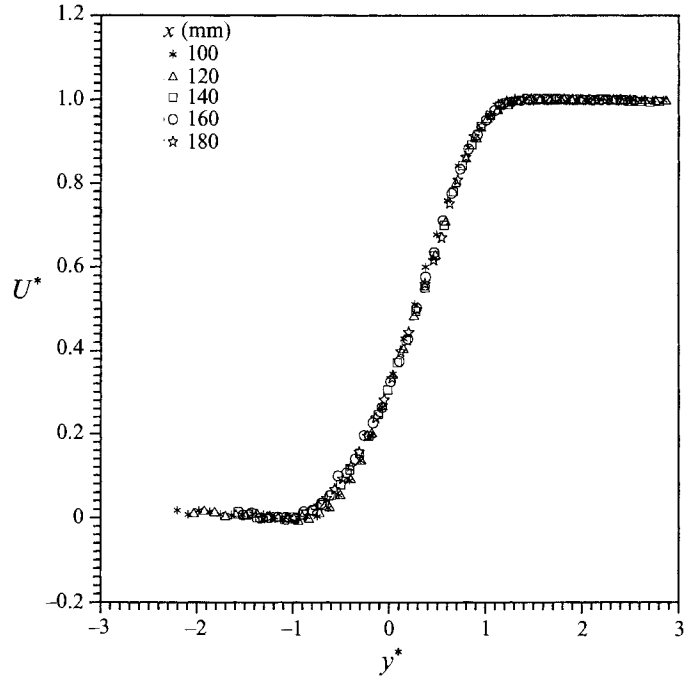

FIGURE 4. Dimensionless mean velocity profiles.

M_e	δ (mm) ($0.995U_e$)	δ^* (mm)	θ (mm)	H	C_f ($\times 10^3$)	u_τ (m s^{-1})	τ_w (N m^{-2})
1.79	9.7	2.18	0.78	2.79	2.02	19.2	45.22

TABLE 2. Characteristics of the explored boundary layer (Quine 1990)

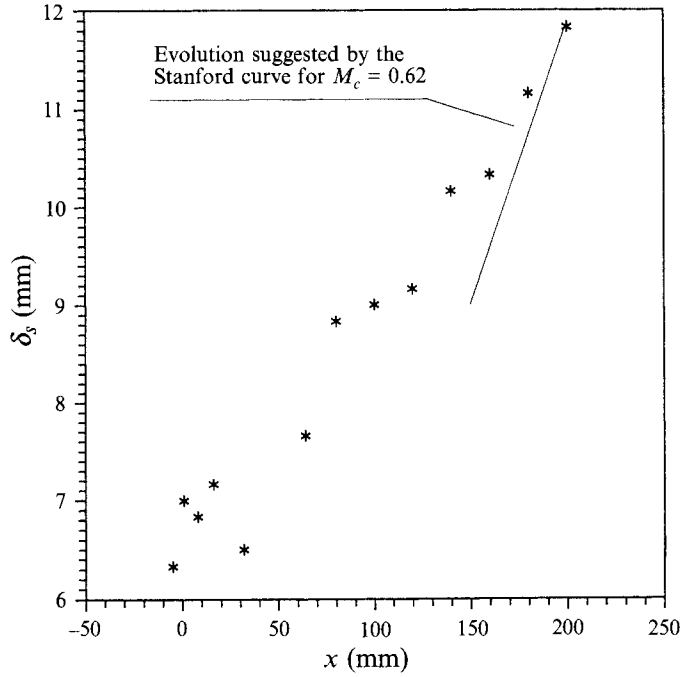

FIGURE 5. Streamwise growth of the 'Stanford' thickness.

Detailed studies of the fluctuating field have been performed, for example by Dzioma & Fiedler (1985) and by Bell & Mehta (1990). They all conclude that the initial development of a mixing layer is controlled to a large extent by the perturbations of the initial boundary layer. In particular Bell & Mehta pointed out that, when the upstream boundary layers are turbulent, no organized structures with longitudinal vorticity can be observed. Such a phenomenon, if it occurs also in supersonic flows, can be important for the development of the three-dimensionality of turbulent structures, which can be enhanced by high speeds. The definition of the initial conditions is then important. In the present cse, on one side of the plate the boundary layer is turbulent. On the other side, the boundary layer is very thin and certainly laminar. At the trailing edge the chamfer angle is 10°, and is probably important for the flow evolution in the first few millimeters downstream of the edge.

Figure 4 presents dimensionless velocity profiles of $U^* = (U-U_2)/(U_1-U_2)$ as a function of $y^* = (y-y_2)/(y_1-y_2)$. The edges of the layers were defined according to the recommendations of the Stanford Conferene (Kline, Cantwell & Lilley 1980), that is y_1 (resp. y_2) is the point where $U = U_2+0.9^{\frac{1}{2}}(U_1-U_2)$ (resp. $0.1^{\frac{1}{2}}(U_1-U_2)$). It appears that near the end of the measurement region the dimensionless profiles collapse with very small scatter, suggesting that the mean fields are approaching similarity.

The longitudinal evolution of the mixing-layer thickness $\delta = y_1-y_2$ is plotted in figure 5. The corresponding spreading rate near the end of the measurement sections has been compared to the so called 'Langley curve' proposed by Birch & Eggers (1973) and retained by P. Bradshaw for the Stanford Conference (Kline *et al.* 1980). It resulted from a compilation of the available mixing-layer spreading rate data (Kline *et al.* 1980). Newer data have been obtained by other authors (see for example Bogdanoff 1983; Chinzei *et al.* 1986; Papamoschou & Roshko 1988 for a review). These results are in satisfactory agreement with each other (figure 19), so that we can keep the Langley curve as a useful consensus. The more recent contributions to these

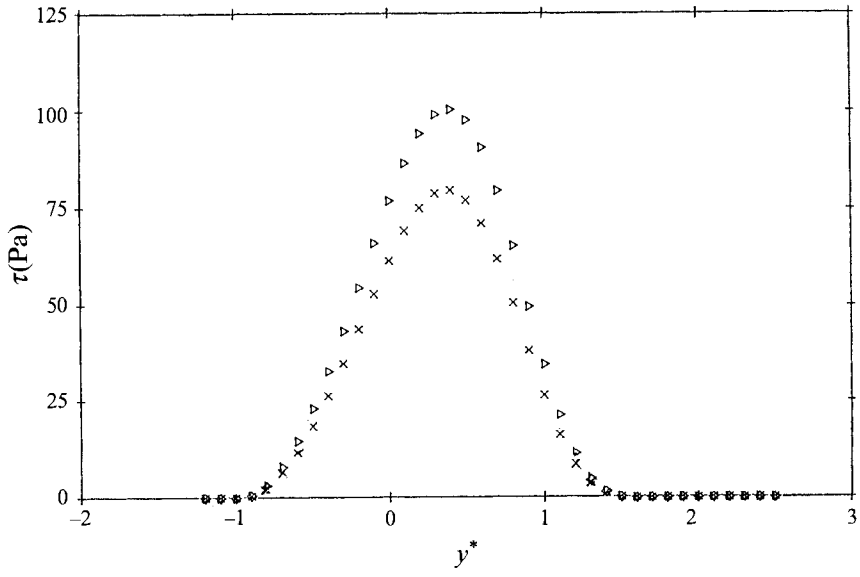

FIGURE 6. Turbulent friction in the developed mixing layer for extreme values of the spreading rate ($x = 180$ mm).

studies, including turbulence measurements, will be included and discussed in §4.2. The present result is below the curve ($\delta' = 0.0338$ for $M_c = 0.62$), suggesting that the asymptotic development of the layer is just being reached. Note that the interpretation may depend on the definition of δ. However, it has been shown (Quine 1990) that the thickness defined using the Pitot profiles is in excellent agreement with the results of Papamoschou (1986).

The turbulent shear stress was deduced from the mean measurements using the mean momentum equation with the assumption that the mean profiles are self-similar. As usual for this method, the longitudinal gradients are rather weak, and can only be determined with questionable accuracy. Several different curve fits were applied to the experimental data to calculate the gradients. This gives some indication of the range of validity of our results. The profiles at $x = 180$ mm are shown in figure 6. The shape of the profile is the expected one; the value of the maximum for the different determinations suggests an uncertainty of $\pm 10\%$ (Quine 1990). The present values will be compared to the results of other authors in §4.

3.3. *Turbulence measurements*

3.3.1. *Measurement method*

The aim of these measurements is to determine the variance of longitudinal velocity $\overline{u'^2}$, of temperature $\overline{T'^2}$ and the correlation coefficient R_{ut} inside and outside the mixing layer. A constant-current hot-wire anemometer was used. As the flow under investigation develops between two streams at Mach numbers of 1.8 and 0.3, the main part of the layer, and particularly the zone where the turbulence intensities reach their maximum, lies in the transonic regime. As indicated by Morkovin (1956) and Horstman & Rose (1977) hot-wire anemometry in transonic flow presents some difficulties. New methods were developed to calibrate the probes and to process the data (Dupont & Debièvre 1989; Barre, Dupont & Dussauge 1992*a*). They are briefly described below.

The characteristic feature of hot-wire heat transfer at transonic speed and at

moderate (and low) Reynolds numbers is that the Nusselt number depends on both the Mach and Reynolds numbers. This implies that the wire is sensitive to mass flux, total temperature *and* Mach number. This causes two difficulties in the measurement procedure. First, calibrations should be performed versus Reynolds and Mach numbers. This has been done extensively, as described in Barre *et al.* (1992*a*) who give the Nusselt number *vs.* Mach and Reynolds numbers in the range $0.3 < M < 1.5$ and $6 < Re_{dt} < 28$. Re_{dt} is the Reynolds number obtained in terms of the local mean mass flux ρu, the viscosity μ measured at the local total temperature and the wire diameter d: $Re_{dt} = (\rho u d)/\mu$. The sensitivity coefficients were deduced according to classical formulae (Morkovin 1956). The results showed that the Mach-number sensitivity coefficient depends strongly on Reynolds number if $Re_{dt} < 15$, which corresponds to the main part of the flow. It was also found that the range of transonic effects is roughly $0.3 < M < 1.3$. However, at lower Reynolds numbers ($Re_{dt} \approx 10$), the effects of Mach number may be ignored for $M > 1$, while for $Re_{dt} \approx 20$, the coefficients of sensitivity to Mach number are smaller, but have significant values up to $M \approx 1.3$. Second, the voltage fluctuation across the wire is

$$\frac{e'}{\bar{E}} = F_{\rho u}\frac{(\rho u)'}{\overline{\rho u}} + F_m\frac{M'}{\bar{M}} + G\frac{T_t'}{T_t}. \tag{5}$$

Squaring this expression and taking the average would produce a relation similar to Kovasznay's (1953) fluctuation diagram. If $F_{\rho u}$, F_m and G were linearly independent functions of overheating, it would be possible to measure the variances of mass flux, Mach number and total temperature. Unfortunately, over a large range of wire overheats $F_{\rho u}$ and F_m are nearly proportional. The determination of the r.m.s. values $\langle(\rho u)'\rangle$ and $\langle T_t'\rangle$ requires further assumptions. It appears that it is more convenient to rewrite equation (5) by introducing the pressure fluctuations instead of the Mach number fluctuations, through the linearized expression:

$$\frac{M'}{\bar{M}} = \frac{1}{2(\alpha+\beta)}\left[(2\alpha+\beta)\frac{(\rho u)'}{\overline{\rho u}} + \frac{T_t'}{T_t} - (2\alpha+\beta)\frac{p'}{\bar{p}}\right], \tag{6}$$

where $\alpha = (1+\frac{1}{2}(\gamma-1)M^2)^{-1}$ and $\beta = (\gamma-1)M^2\alpha$.

The pressure fluctuation has to be specified. Examples are given below for two particular cases of practical interest. First, in shear flows where vorticity is strong, the 'no sound' assumption is used, as in Kovasznay (1953) and Dupont & Debiève (1989): $p'/p \ll \rho'/\rho$. Pressure fluctuations are neglected in (6), and the fluctuation voltage becomes

$$\frac{e'}{\bar{E}} = F_1\frac{(\rho u)'}{\overline{\rho u}} + G_1\frac{T_t'}{T_t},$$

where

$$F_1 = F_{\rho u} + \frac{(2\alpha+\beta)}{2(\alpha+\beta)}F_m, \quad G_1 = G + \frac{1}{2(\alpha+\beta)}F_m.$$

It is then possible to measure $\langle(\rho u)'\rangle$, $\langle T_t'\rangle$ and their correlation coefficient $R_{\rho u, T_t}$ and to deduce $\langle u'\rangle$, $\langle T'\rangle$, and R_{ut} using the classical method.

This assumption ($p'/p \ll \rho'/\rho$), which is valid in zero-pressure-gradient subsonic and supersonic boundary layers, has also been used for our mixing layer. It has been verified by Barre *et al.* (1992*a*) that this method is suitable for measurements in the initial boundary layer and in the mixing layer (see §3.3.2 and figure 8).

The second case under examination corresponds to external flows, where data reduction should be performed by the method proposed by Laufer (1961). In this

situation pressure fluctuations induced by turbulent eddies are significant, the acoustic mode is predominant, and the correct approximation consists in assuming that pressure, temperature and density fluctuations are linked by isentropic relations:

$$p'/\bar{p} = \gamma\rho'/\bar{\rho} = (\gamma/(\gamma-1))\,T'/\bar{T}.$$

The Mach number fluctuations are

$$\frac{M'}{\bar{M}} = \frac{(2\alpha+\beta)}{2(\alpha+\beta)}\left[1-\frac{\beta\gamma}{(1-\gamma)\alpha+\beta}\right]\frac{(\rho u)'}{\overline{\rho u}} + \frac{1}{2(\alpha+\beta)}\left[1+\frac{\gamma(2\alpha+\beta)}{(1-\gamma)\alpha+\beta}\right]\frac{T_t'}{\overline{T}_t}. \tag{7}$$

Then the voltage fluctuation can be expressed as

$$\frac{e'}{\bar{E}} = F_2\frac{(\rho u)'}{\overline{\rho u}} + G_2\frac{T_t'}{\overline{T}_t},$$

with

$$F_2 = F_{\rho u} + \left[\frac{(2\alpha+\beta)}{2(\alpha+\beta)}\left[1-\frac{\beta\gamma}{(1-\gamma)\alpha+\beta}\right]\right]F_m,$$

$$G_2 = G + \left[\frac{1}{2(\alpha+\beta)}\left[1+\frac{\gamma(2\alpha+\beta)}{(1-\gamma)\alpha+\beta}\right]\right]F_m.$$

In the present case, the Mach number of the high-speed side is $M_1 = 1.8$, so that $F_m = 0$, $F_2 = F_{\rho u}$ and $G_2 = G$. Then Laufer's method remains unchanged. On the low-velocity side $M_2 = 0.3$ and the contribution of F_m again seems negligible. It is then possible to determine $\overline{u'^2}$, $\overline{p'^2}$ and their correlation coefficients in the external flows.

Moreover, in the supersonic external flow, the velocity of the sources of aerodynamic noise may be measured as described by Laufer (1961). This method assumes that the pressure fluctuations in the outer flow are isentropic. If they are produced by plane Mach waves it is possible to determine the speed of the sources. Although there is no obvious relationship between the convective velocity of the large-scale structures of the layer and the source speed, it was hoped that this parameter could give an indication on the dynamics of the energetic turbulent vortices (see §3.3.3 for further discussion).

3.3.2. *Characteristics of the anemometer*

The hot-wire probe was made of a tungsten wire of 5 μm in diameter welded to the prongs. The probe was a standard Dantec probe type No. 55P11; its stiffness was enhanced by putting a drop of glue between the prongs. The aspect ratio of the wire was 240. In the external flows and on the edges of the layer, it was checked that the wire was not affected by vibrations. In the middle of the layer, the turbulence intensities are high and induce a strong excitation on the wire, making it difficult to have a wire free from strain gauge effects. For the present measurements, an estimate of the error has been made from the spectra of the signal. It showed that the contribution of this effect is about 15% to $\langle u' \rangle$, at the maximum of the turbulence intensity. The time constant of the wire was measured *in situ* by the square-wave method as described in Arzoumanian & Debiève (1989). In this method the wire response to a square wave is recorded by an HP computer after being low-pass filtered at 35 kHz. The resulting signal was phase averaged over the period of the square wave in order to eliminate the spurious turbulent component superimposed on the response. Exponential curves were then fitted by a least-squares method. The value of the time constant was then deduced. This procedure proved to be efficient: it saved time, it was repeatable and avoided the subjective aspect of the visual setting. The bandwidth of the compensated anemometer was 200 kHz. If structures of wavelength δ are convected at velocity U_c, they produce

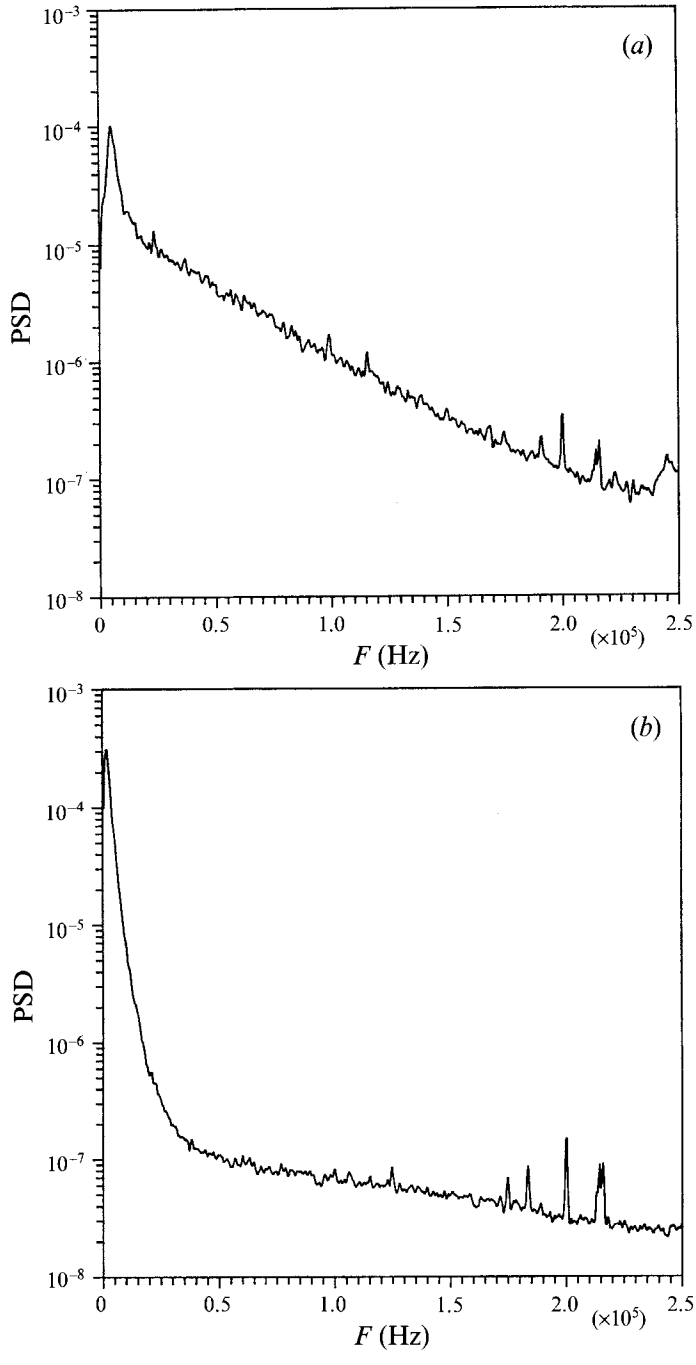

FIGURE 7. Power spectral density measured in the mixing layer (high-pass filter = 1 kHz, overheating ratio = 0.4) at $x = 64$ mm. (*a*) $y = 12$ mm, (*b*) $y = -20$ mm.

a characteristic frequency U_c/δ of about 15 kHz in our case. The cutoff of the electronics is therefore about 13 times the characteristic frequency, and more than adequate to measure the energy of the signal in shear flows according to Kistler's criterion (Kistler 1959; Smits & Dussauge 1989). Finally, the fluctuation diagram was determined by measurements at 14 overheats, ranging from zero to 0.45.

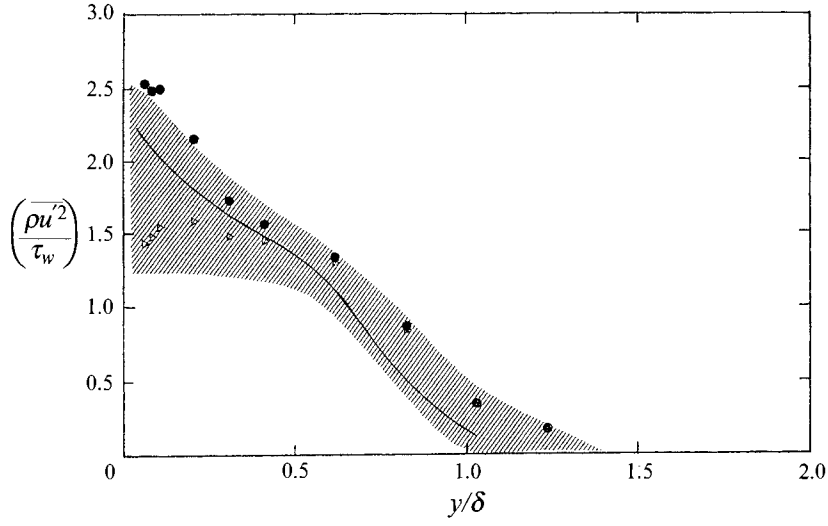

FIGURE 8. Velocity fluctuation measurements in the initial boundary layer: influence of the sensitivity coefficient on Mach number: △, $F_m = 0$; ●, $F_m \neq 0$; ——, Klebanoff's (1955) data, $M = 0$; shaded zone, range of the available velocity fluctuation data in supersonic boundary layers, including hot-wire and laser-Doppler measurements.

3.3.3. *Experimental results*

In this subsection, three sets of results are presented: the fluctuations in the initial flows, turbulence measurements in the mixing layer, and the longitudinal evolution of the induced fluctuations in the outer flows.

Just downstream of the trailing edge, at $x = 1$ mm, the r.m.s. value of the velocity fluctuations is 1.14 m s^{-1} in the supersonic flow and 3.8 m s^{-1} in the subsonic flow. This gives $(\langle u' \rangle / \Delta U) = 0.3\,\%$ and $(\langle u' \rangle / \Delta U) = 1\,\%$ respectively for the outer and the inner flows. These values correspond to practically the same intensity of pressure fluctuations in both flows, $\langle p' \rangle / \bar{p} \approx 1\,\%$.

In the inner flow, turbulence is generated as it enters the tunnel by the plate of porous bronze (see figure 1*a*). This turbulence decays between the base and the trailing edge and it was checked that $(\langle u' \rangle / \bar{U})^2$ decays proportionally to $1/x$, as for grid-generated turbulence (see for example Hinze 1959).

Spectra of the hot-wire signal were measured in both external flows, at $x = 64$ mm (figures 7*a* and 7*b*), at an overheat ratio of 0.4, so that the signal is nearly proportional to the mass flux fluctuation. The range of frequencies involved in the supersonic and in the subsonic flows is rather different. As expected, higher frequencies are found in the supersonic flow, but in both cases broadband spectra without peaks are observed: the mixing layer is not excited at a particular frequency.

Velocity measurements were performed in the initial boundary layer. They are presented in Morkovin's representation in figure 8, where τ_w is the wall friction. They show very clearly that the transonic calibration is very important in the present case: processing the data with Mach-number effects produces significant differences for $M < 1.3$. The largest error is observed near the wall, where $M \approx 1$, and reached 40% for $\langle u' \rangle$. The results are in excellent agreement with previous data of other authors, confirming that the initial boundary layer on the high-velocity side is turbulent and fully developed.

Figure 9 presents the profiles of the r.m.s. velocity fluctuations $\langle u' \rangle$ in the mixing

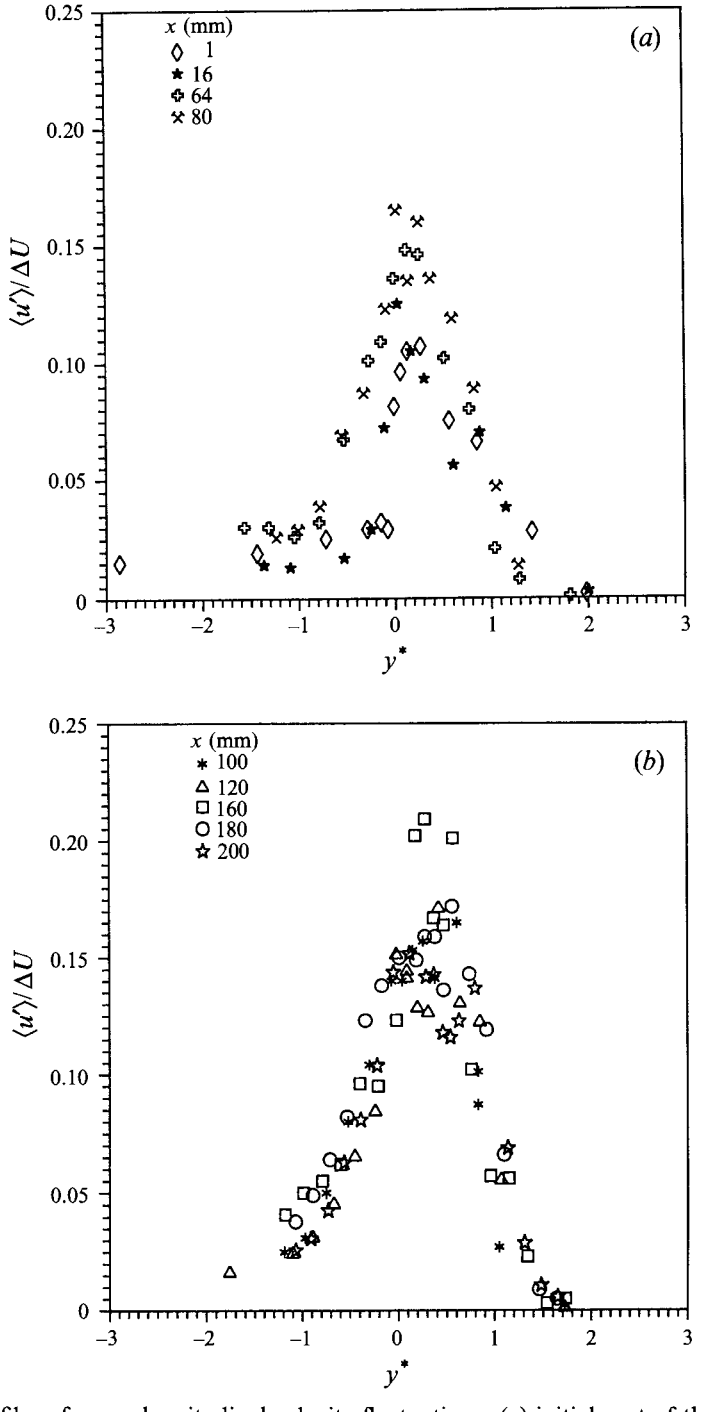

FIGURE 9. Profiles of r.m.s. longitudinal velocity fluctuations: (*a*) initial part of the mixing layer, (*b*) mixing layer approaching asymptotic state.

layer, normalized by the velocity difference across the layer, $\Delta U = U_1 - U_2$. Again, the longitudinal evolution can be seen: the flow starts with profiles corresponding to an equilibrium boundary layer and in the last sections the shape corresponds to a mixing layer. There is a rapid increase in the fluctuation level up to $x = 100$ mm, but

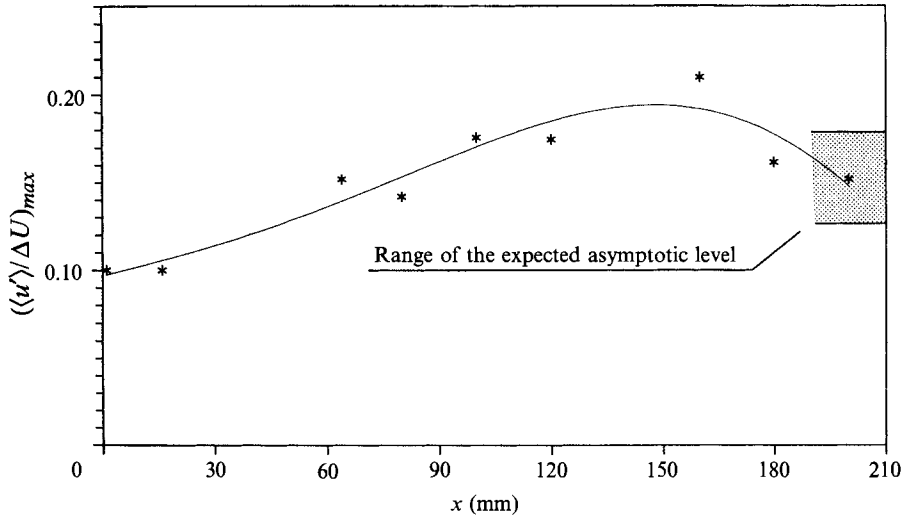

FIGURE 10. Streamwise evolution of the maximum r.m.s. velocity fluctuations.

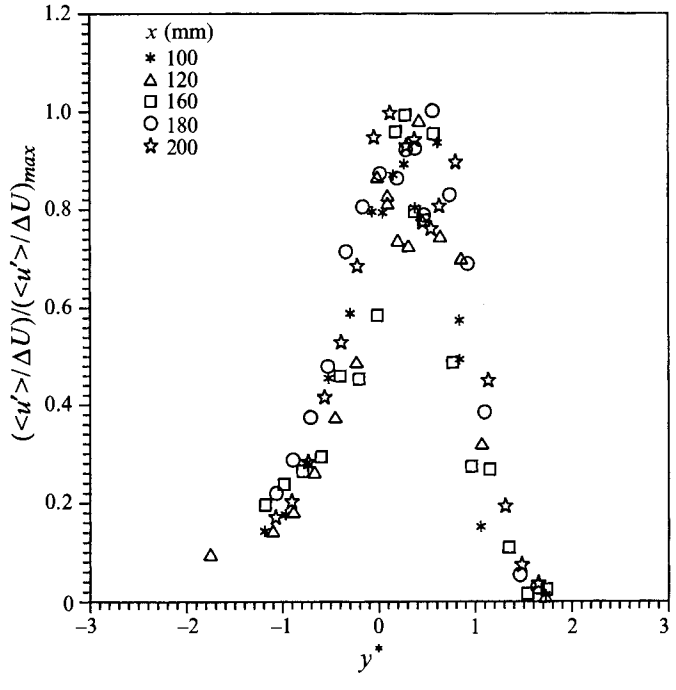

FIGURE 11. Similarity test on the velocity turbulence intensity.

downstream the evolutions become weaker. A more careful examination reveals an overshoot in the maximum level, near $x = 160$ mm. This is illustrated by figure 10 where the maximum values *vs.* longitudinal distance are shown. They are compared with an asymptotic level, deduced from a compilation of the existing data (figure 21) which will be discussed in §4. Anticipating this analysis suggests that the mixing layer is practically fully developed. This seems to be confirmed by the evolution of the shape of the profiles when normalized by the maximum value at each location (figure 11). There is still some scatter which, to some extent, may hide the trends, but the tendency

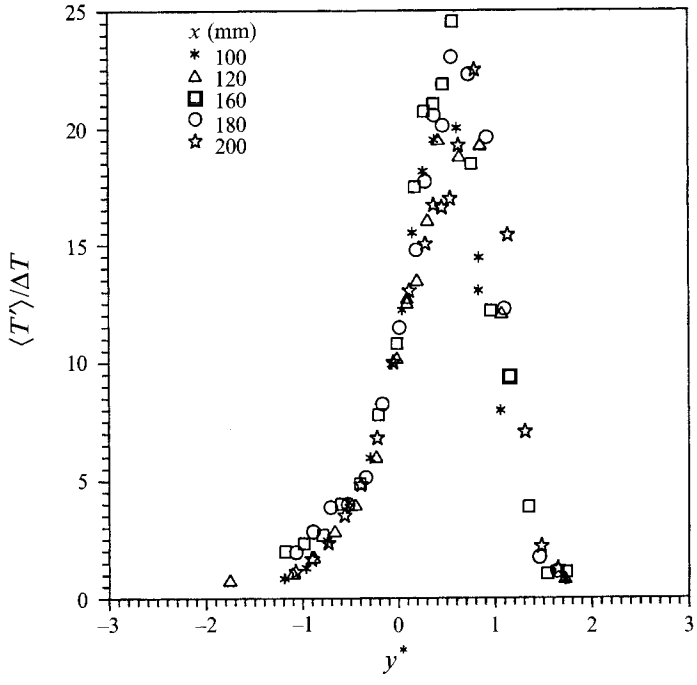

FIGURE 12. Temperature fluctuations in the developed part of the mixing layer.

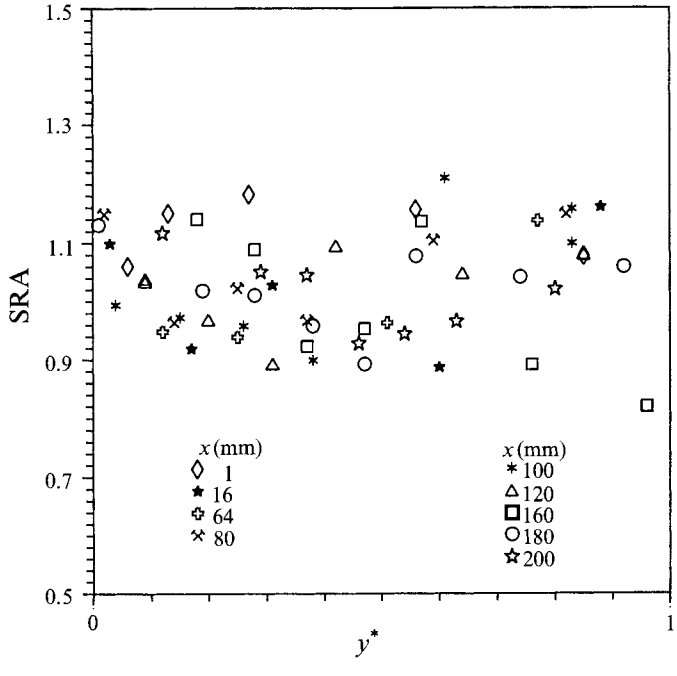

FIGURE 13. Verification of the strong Reynolds analogy relation.

seems to be a collapse of the data at the last three measurement stations. Similar evolutions are observed in the measurements of the temperature fluctuation intensity $\langle T' \rangle / \Delta T$ (figure 12) where $\Delta T = T_1 - T_2$. From the present results it is possible to check whether the result of the Strong Reynolds Analogy (SRA) still holds (Morkovin 1962;

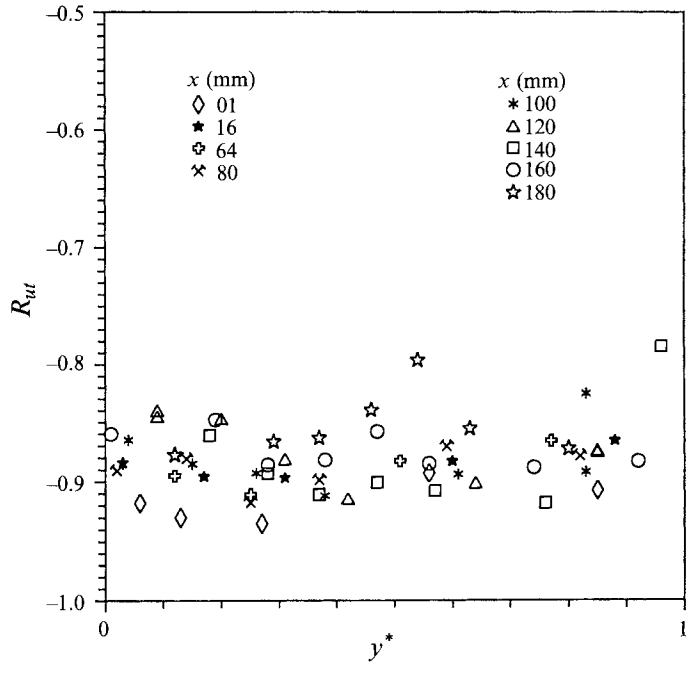

FIGURE 14. Velocity–temperature correlation coefficient.

Gaviglio 1987). The result is given in figure 13 for the central part of the layer where SRA is the ratio:

$$\text{SRA} = (\gamma - 1)\, M^2 \frac{\langle u' \rangle / \bar{U}}{\langle T' \rangle / \bar{T}}. \tag{8}$$

Near the edges of the mixing layer, because of the intermittency, the assumptions used to reduce the data are more crude and the results are less reliable. The analogy corresponds to the value SRA = 1, and to a velocity–temperature correlation coefficient equal to -1. It appears that this relationship seems to hold well, as in other supersonic flows without heat sources. A sufficient condition to obtain relation (8) is that the total enthalpy flux is small compared to the enthalpy flux (Morkovin 1962), and as our flow included no heat sources, it is not surprising to find that the SRA ratio remains practically equal to unity. The correlation coefficient (figure 14) supports this interpretation: it is remarkably constant in the layer and has a value near -0.9.

Finally, the r.m.s. pressure fluctuations $\langle p' \rangle / \bar{p}$ were measured in the external flows (figure 15). On both sides of the layer, there is an increase in the r.m.s. pressure level, reaching a maximum in the vicinity of the maximum of the velocity fluctuations. From the measurements of $\langle p' \rangle / \bar{p}$ in the external flow it is possible, using Laufer's method (Laufer 1961), to deduce the speed of the aerodynamic noise sources involved in this flow. The main points of this method can be briefly summarized as follows. Since the external flows can be presumed isentropic, we use the following assumption:

$$p'/\bar{p} = \gamma(\rho'/\bar{\rho}) = (\gamma/(\gamma - 1))(T'/\bar{T}).$$

This equation shows that the intensity of the entropy mode is negligible in the external flows (Kovasznay 1953).

Moreover, if we assume that the fluctuation field in the external flow is a 'pure sound field' giving a pressure–velocity correlation coefficient of $\pm 1 (R_{up} = \pm 1)$ and that it

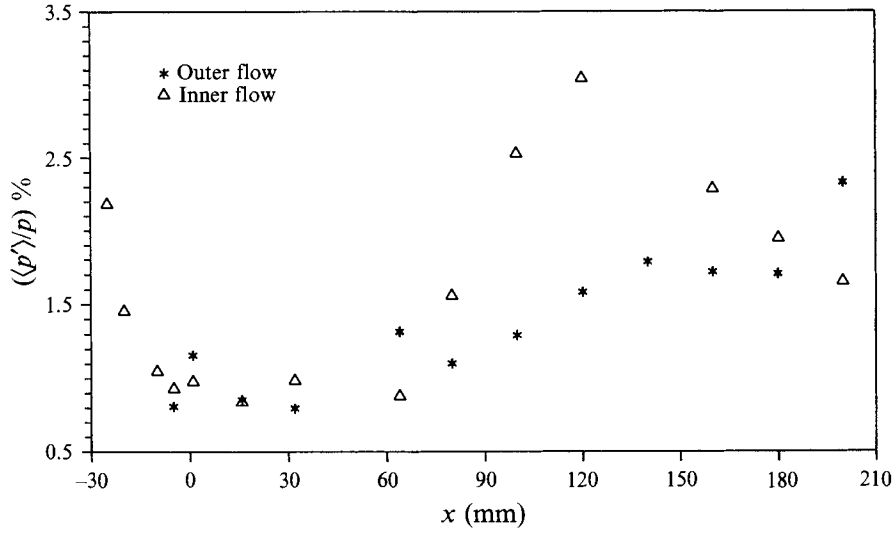

FIGURE 15. Pressure fluctuations level in both external flows.

corresponds to plane sound waves, we can find a relation between velocity and pressure fluctuations:

$$u'/U = (\cos\theta M)(p'/\gamma p),$$

where θ is the angle between the normal to the wave front and the direction of the mean flow; M is the local mean Mach number.

It is now possible to calculate a mean orientation of the waves and, in turn, to obtain a mean propagation velocity of the sound sources U_s since

$$(U-U_s)/a = -1/(\cos\theta);$$

a being the local speed of sound we can easily write

$$\frac{U_s}{\bar{U}} = 1 \pm \frac{1}{M\cos\theta} = 1 \pm \frac{\langle p'\rangle/\gamma\bar{p}}{M^2\langle u'\rangle/\bar{U}}.$$

On the supersonic side, the speed of the sources of aerodynamic noise U_s was deduced from the hot-wire measurements (figure 16). In the initial boundary layer the ratio U_s/U_e is about $\frac{1}{3}$; this value is in good agreement with Laufer's (1961) results for equilibrium supersonic boundary layers at $M = 1.8$. Further downstream, U_s decreases and has a value of about $100\ \mathrm{m\ s^{-1}}$ for $x > 100$ mm. Then it seems that the perturbations producing the most significant part of the plane wave noise radiated into the supersonic flow travel with a velocity of the order of the velocity of the subsonic flow.

In fact, in the present flow, where compressibility effects are weak ($M_c = 0.62$), it is possible to assume that large structures are convected at a subsonic Mach number with respect to the external flows. So, the acoustic perturbations due to the convection of these eddies are probably waves with exponential decay and not plane Mach waves. It is not very surprising to find U_2 as the noise source velocity because ΔU is of the order of the sound speed in this layer, making the subsonic flow (flow 2) the most significant plane Mach wave source detectable with the present measurement method when the

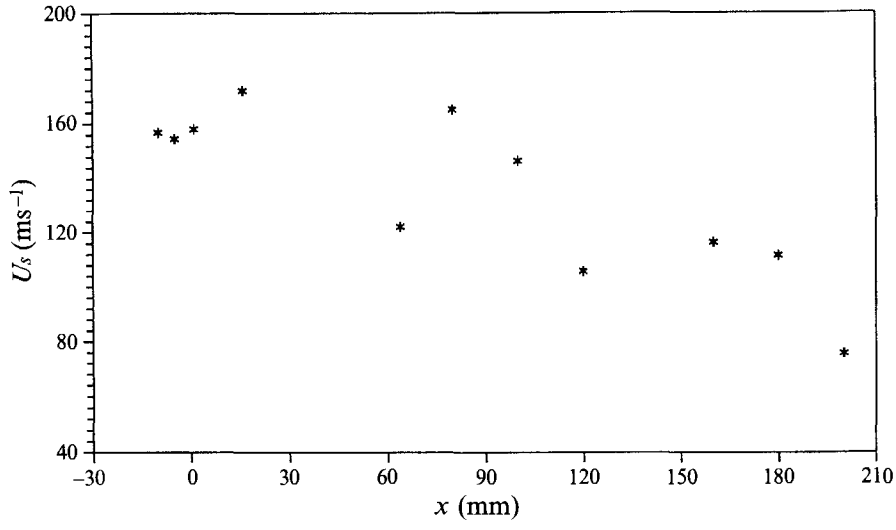

FIGURE 16. Velocity of the noise sources.

hot-wire probe is placed in the supersonic free stream. In a more compressible mixing layer with M_c greater than unity, this method would probably be appropriate for obtaining the convection velocity of the large eddies because the most significant plane sound wave sources in such a flow are the large eddies. This has been investigated by Hall (1991) with an optical method.

On the subsonic side the situation was not so clear because of the sound field superimposed on the incoming turbulence in the secondary flow. The intensity of these vortical fluctuations was at least as large as the fluctuations radiated by the eddies. This made the present method inappropriate for the determination of U_s on the subsonic side.

4. Discussion

4.1. *The development of the mixing layer and its sensitivity to initial conditions*

Mixing layers are flows which are very sensitive to initial and boundary conditions. In the present study, the first evidence of a self-similar state was found from the mean density profiles at the last stations, at a distance from the trailing edge of about 350 times the initial momentum thickness. It seems difficult to predict the distance required for supersonic shear layers to become fully developed, but Dutton *et al.* (1990) proposed a criterion based on the Reynolds number $Re = \Delta U\delta/\nu$, where ν is the average kinematic viscosity. They found from their experiments that the flow is fully developed when Re is approximately 10^5. Our results agree with this criterion, since $Re \approx 1.6 \times 10^5$ at the last stations of our measurements.

The full development of the layer seems to be reached after an overshoot on the maximum of $\langle u' \rangle$, located at a point coinciding with an increase of the r.m.s. pressure level, but the reasons for this overshoot are not well understood. The schlieren photograph and the wall pressure measurements (figure 1*a* and 1*b*) suggest that no undesired wave system can explain the observed overshoot. A more precise investigation of this point was made by inspection of the static pressure profiles (figure 17). It appears that in all the sections there is a slight imbalance of pressure between

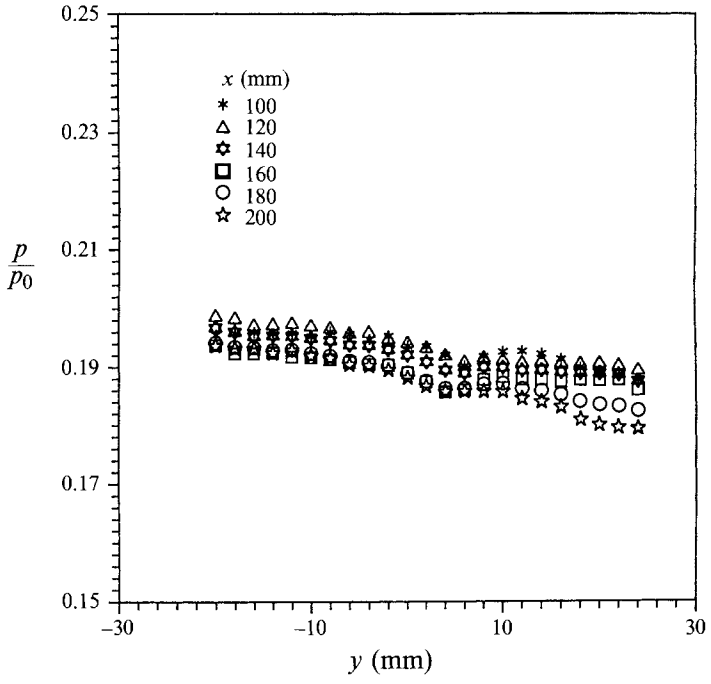

FIGURE 17. Static pressure profiles for the final part of the mixing layer (pressure related to stagnation condition).

the supersonic and the subsonic flow, typically 2%. This difference is observed in all sections. So the overshoot of the r.m.s. velocity cannot be explained by an interaction of the layer with a parasitic wave. By reference to the phenomena usually related to mixing layers, it may be speculated either that some pairing is occurring, or that the layer experiences compressibility effects and the energetic structures become highly three-dimensional. Further discussion will be given in §4.2.

It was also checked that the final level does not depend on the initial conditions. When large V-shaped roughnesses (0.7 mm high commercially available DEMO tape) were put on the plate on the low-velocity side to perturb significantly the thin (laminar) boundary layer, it was found that, within the range of accuracy of the measurements, no effect on the level of $\overline{u'^2}$ at $x = 160$ mm, was observed (see figure 18*a*). This confirms the high level of fluctuations found in this section. Similarly, it was suspected that possible three-dimensional effects could be triggered by turbulent perturbations coming from the sidewall. To check this effect, inclined plates were put on the sidewalls at the trailing edge and formed a 7° divergent. They were supposed to modify the evolution of the boundary layer by changing the perturbation at the junction between the sidewalls and the trailing edge. The results at $x = 120$ mm (see figure 18*b*) showed no sensitivity to this modification of the initial conditions. It was concluded that, if the r.m.s. velocity fluctuations are considered, the final state, corresponding to the fully developed state, was virtually independent of the initial conditions.

4.2. *Discussion on the compressibility effects*

A compilation of the available normalized spreading rate data calculated with equation (2) is shown in figure 19 where we have plotted the Langley curve and the experimental values of $\phi(M_c)$ deduced using the isentropic estimates of U_c in (2). In this

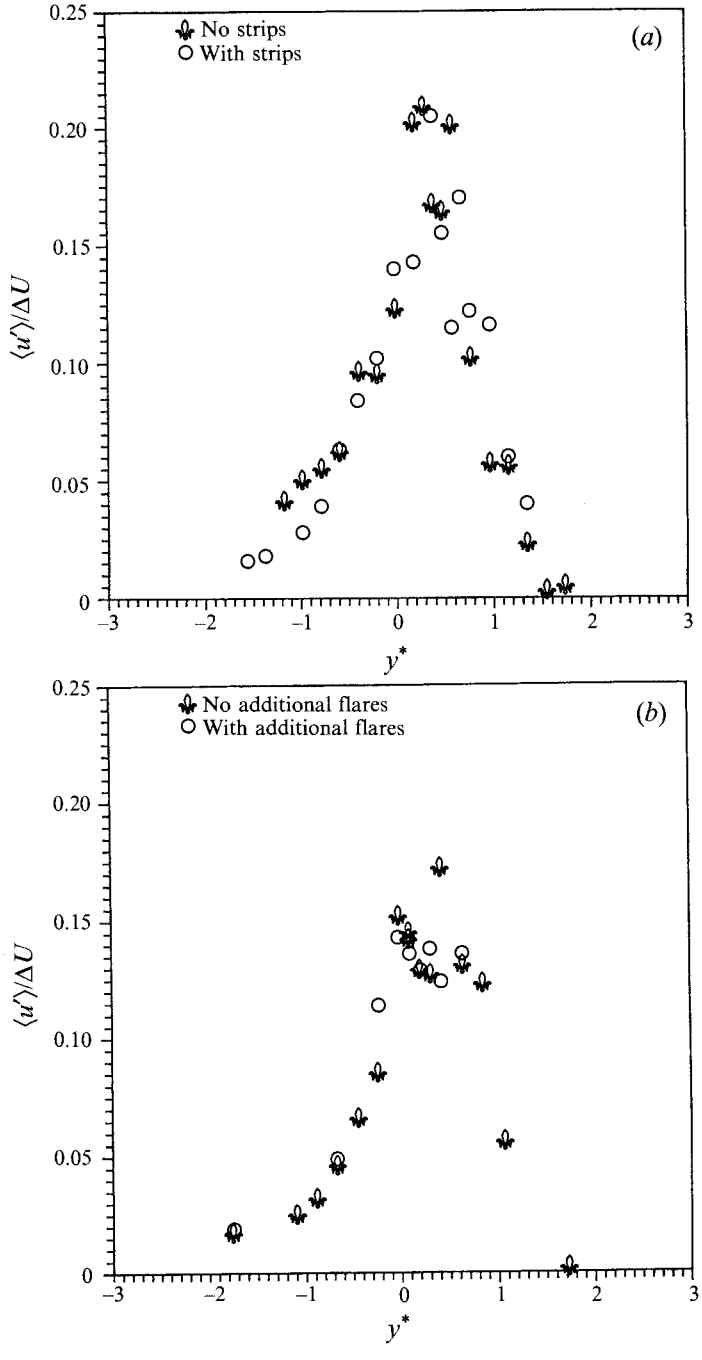

FIGURE 18. (*a*) Effects of strips on longitudinal velocity fluctuations (x = 160 mm). (*b*) Effects of additional flares on longitudinal velocity fluctuations (x = 120 mm).

representation, as recalled in §2, $M_c = \Delta U/(a_1 + a_2)$ is kept as the parameter characterizing the compressibility effects. The overall agreement seems quite close to the Langley consensus except for some flows like the present experiment and also that of Debisschop (1993). This discrepancy will be discussed later in this section by comparison with the turbulent diffusion model proposed in equations (3) and (4). It

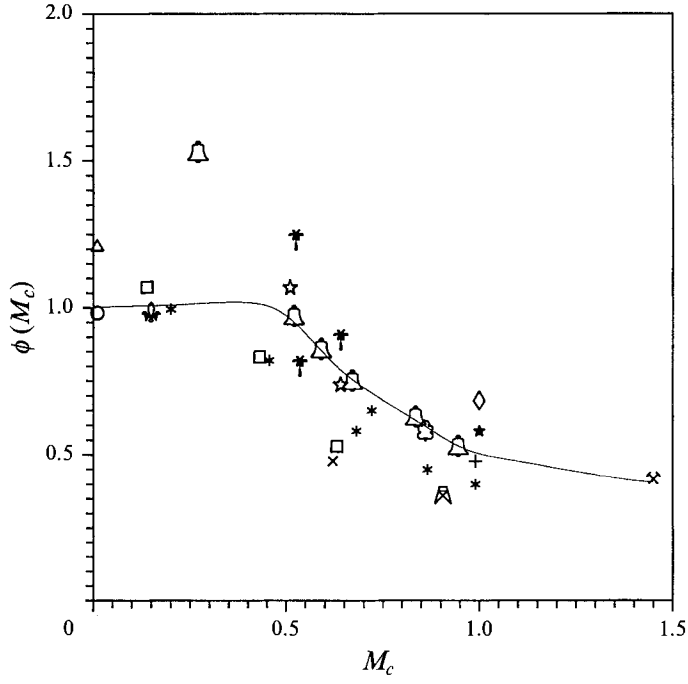

FIGURE 19. Variation of the measured normalized spreading rate by different authors: ⏢, Elliott & Samimy (1990); ✝, Debisschop (1993); ⚜, Bradshaw (1966); ○, Liepmann & Laufer (1947); □, Lau (1981); △, Wygnanski & Fiedler (1970); ◇, Samimy, Petrie & Addy (1986); 🙏, Hall (1991); ☆, Samimy & Elliott (1990), +, Ikawa & Kubota (1975); ×, present result; ∗, Dutton *et al.* (1990); ★, Petrie, Samimy & Addy (1986); ⚒, Wagner (1973); ⏢, Chinzei *et al.* (1986); solid line, 'Langley curve'.

may be remarked that Chinzei *et al.*'s (1986) data show an excellent agreement with the Langley correlation except for their case at $M_c = 0.25$ where, probably, the flow is not completely developed.

The measured level of turbulent friction obtained in the present experiment has been compared to the results of the other authors as shown in figure 20, which presents $(-\overline{u'v'})_{max}/(\Delta U)^2$ as a function of M_c. Note that, at low Mach numbers, some high values of the shear stress are observed: the data point from Dutton *et al.* (1990) at $M_c = 0.2$ is too high, but this flow is perhaps not completely developed and is probably more a wake than a mixing layer (Dutton, private communication, 1991). The laser measurements by Lau, Morris & Fisher (1979) are too high, as noticed by the authors themselves. An assessment of the systematic error can be deduced from Lau (1981) by accepting their corrections on $\overline{u'^2}$ and their comparisons with hot-wire measurements. The results plotted in figure 20 take this effect into account. However the resulting value for $M_c = 0.15$ is higher than the average level. It can be seen that the present shear stress is below the trend of the other measurements. This shear stress value is deduced from the mean measurements by the mean momentum balance. The method leads to an uncertainty of $\pm 10\%$ (see §3.2 and Quine 1990), which, therefore cannot explain the observed discrepancy. Although the mean velocity profiles are self-similar and have the usual shape, the layer is perhaps just reaching the asymptotic state: turbulence data are generally more sensitive to this effect than mean quantities and perhaps have not reached the asymptotic value. Another element of explanation is that in our experiment the turbulence level of the external flows is probably lower than in

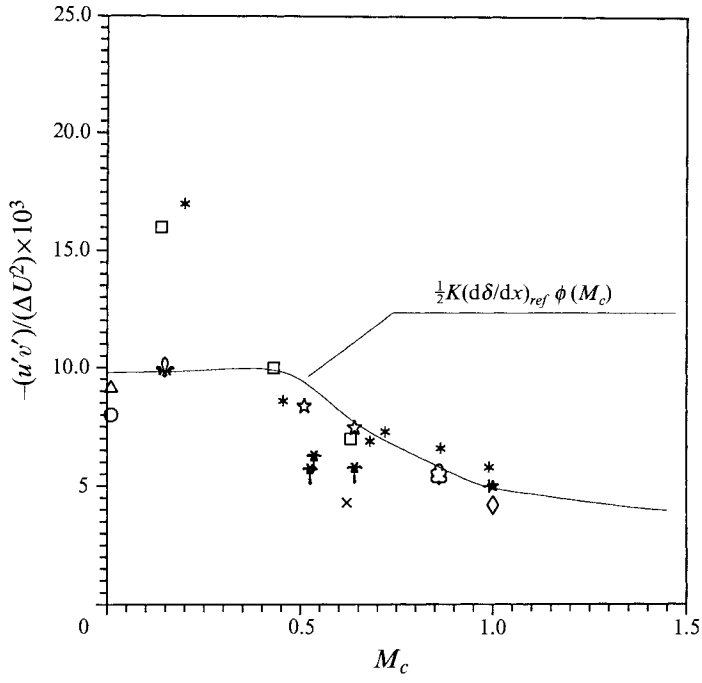

FIGURE 20. Variation of the measured dimensionless turbulent shear stress by different authors (see figure 19 for legend). The solid line represents the shear stress deduced from the spreading rates of the 'Langley curve' using $K = 0.17$ in equation (4).

the others considered in the present compilation. It was felt however that this fact could not explain entirely the observed discrepancy. A last possible explanation is that these different flow cases cannot be compared in such a straightforward way. Equation (4) suggests that the density ratio can affect the turbulence level through K. This was examined for the present flow cases. It appears that most of the supersonic flows considered in figure 20 have a density ratio close to 0.6, so that the influence of this parameter in figure 20 cannot be large.

Finally, relations (3) and (4) were used as possible guides for interpreting the results. Our low friction level then seems consistent with the rather low value of the spreading rate which was deduced from the present experiment (see figure 19). These two measured values have been used together with relation (3) to determine K assuming that the isentropic estimation of U_c is a convenient choice since the present convective Mach number is not high ($M_c = 0.62$). The resulting value obtained for K is 0.16, which is close to the one obtained in subsonic experiments (0.17 for Bradshaw 1966, 0.13 for Wygnansky & Fiedler 1970 and 0.14 for Liepman & Laufer 1947). It can be noticed from Nottmeyer's (1990) and Fiedler *et al.*'s (1990) results, for a density ratio in the range ($0.6 \leqslant s \leqslant 1$), that the influence of s on K is rather low and not strong enough to change significantly the observed agreement on K between low-speed flows (Nottmeyer 1990; Wygnanski & Fiedler 1970; Liepmann & Laufer 1947) and the present experiment. So, considering this agreement on K, (4) has been used to illustrate this. Figure 20 shows the computed variations of $(\overline{-u'v'})_{max}/(\Delta U)^2$ obtained from relation (4) using $K = 0.17$ and the function $\phi(M_c)$ given by the Stanford consensus ('Langley curve'). The overall agreement is good and it was checked that it was closely achieved for flows whose spreading rate is close to the one given by the Langley consensus (see figure 19).

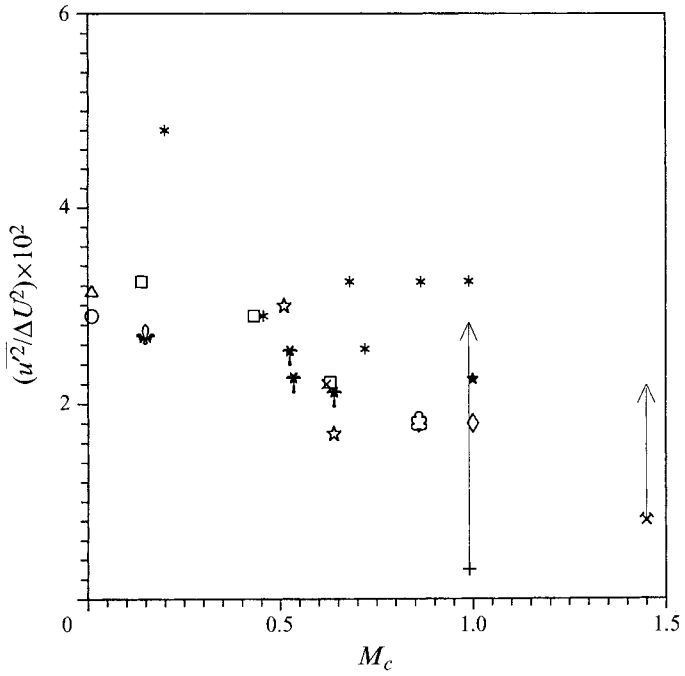

FIGURE 21. Variation of $\overline{u'^2}/\Delta U^2$ as a function of M_c (see figure 19 for legend). Arrows indicate the present reassessment of the measurements.

The conclusion that can be drawn from the results on friction is that supersonic mixing layers can be described adequately by a turbulent diffusion scheme which relates the turbulent friction and the spreading rate. This relation is based on a characteristic diffusion time in a convected frame of reference $K(s, M_c)$. This diffusion time seems nearly independent of the convective Mach number at least up to $M_c = 0.62$. Moreover, if the Langley consensus gives a correct evaluation of the spreading rate of compressible mixing layers, it seems that some flows do not fully agree with this correlation. It has been shown by Dimotakis (1991) that, even in subsonic cases, it is difficult to define an overall consensus on the spreading rate of mixing layers. This is certainly due to the high sensitivity to external conditions of these flows as stated by Bradshaw (1966). However, the present turbulent diffusion scheme seems to be able to describe a large group of mixing layers even if their spreading rate is not in close agreement with the Langley consensus, as in the present case. This diffusion scheme may provide a basis for a better correlation, but need to be investigated for larger convective Mach numbers and for other density ratios.

The examination of $\overline{u'^2}$ is of particular interest, since Smits *et al.* (1989) have shown that in high-speed boundary layers, turbulence anisotropy seems to be changed by compressibility. A better test would be to consider $\overline{v'^2}$, this stress being probably a better indicator of anisotropy modifications. However this quantity could not be measured in the present work. The results on $\overline{u'^2}/\Delta U^2$ are shown in figure 21. As discussed previously for the shear stress, some reservations may be expressed on the generality of such a plot, probably due to the influence of the density ratio s which is not really the same in all flows. Rather unexpectedly, the scatter is larger than for $-\overline{u'v'}$. Concerning Dutton *et al.*'s data for $M_c = 0.2$, the high value is probably due to a lack of flow development as discussed for $\overline{u'v'}$. The present measurements show that $\overline{u'^2}/\Delta U^2$ for $M_c = 0.62$ is lower than in subsonic cases. While the present turbulent

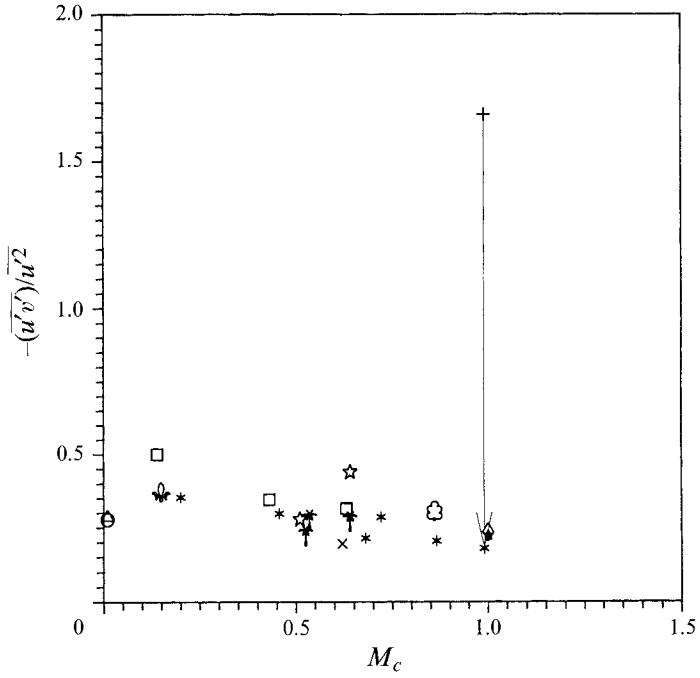

FIGURE 22. Variation of the ratio $(\overline{-u'v'})/\overline{u'^2}$ as a function of M_c (see figure 19 for legend). Arrow indicates the present reassessment of the measurements.

friction was found to be lower than the average of other authors, $\overline{u'^2}/\Delta U^2$ is consistent with most of the supersonic data, excepted those of Dutton *et al.* (1990), and suggest that this quantity decreases with increasing M_c. The ratio $\overline{u'v'}/\overline{u'^2}$ is plotted in figure 22 and is found to be about 0.2 for the present flow case, where the maximum value of $\overline{u'^2}$ in section $x = 200$ mm has been used. The departure from the subsonic value is rather large. However, it is difficult to determine accurately the considered ratio because of a possible accumulation of uncertainties: typical inaccuracies on $\langle u' \rangle$ and on $\overline{-u'v'}$ were estimated at about 10%.

The measured variation is then at the limit of the experimental errors. It is however believed that our results indicate an effect of compressibility on Reynolds stress anisotropy. (It should be mentioned that there is a flaw in figure 4 of Dupont *et al.* 1993, leading to an underestimation of 30% in $\overline{u'^2}$.) The trend indicated by other data is not clear: Dutton *et al.*'s data suggest an increase of $\overline{u'^2}$ and of $\overline{u'^2}/\overline{-u'v'}$, while the data given by Ikawa & Kubota (1975), and Wagner (1973) show the opposite trend. A reassessment of the data of Ikawa (1973) and Wagner (1973) has been performed. It was suspected that there might be some hot-wire transonic calibration effects at the maximum of the turbulence intensity, not taken in account in these two experiments. However, in general the stagnation temperature is barely affected by such conditions (Barre *et al.* 1992*a*). The measured r.m.s. value of the stagnation temperature has therefore been retained. As there are no heat sources in Ikawa's flow, and as the heat fluxes are moderate in Wagner's experiment, it was assumed that the SRA can be applied and that R_{ut} is constant ($R_{ut} = -0.9$). The resulting values of $\overline{u'^2}/\Delta U^2$ and $\overline{-u'v'}/\overline{u'^2}$ are shown in figures 21 and 22 by arrows. Again it is difficult to draw conclusions because our evaluation is very crude and not very accurate, but the maximum reassessed values do not contradict a decrease of $\overline{-u'v'}/\overline{u'^2}$ for large M_c.

However, the apparent agreement of the present measurements with Dutton *et al.*'s results on anisotropy are not obtained for the same reasons: in the present case, this decrease is due to a low value of the shear stress and not to a high value of $\overline{u'^2}$. Additional experiments with well-defined flow conditions and well-controlled measurement methods are needed to answer this question at large convective Mach numbers.

A last finding to be explained is the overshoot in the longitudinal evolution of the maximum of $\overline{u'^2}$ (figure 10); it corresponds to an extremum of $\overline{p'^2}$ in the outer flows. At the location of the overshoot, a more rapid penetration of the shear layer into the low-speed flow is observed from both mean measurements and schlieren visualizations (figure 1*b*). In this zone, it is also more difficult to see large-scale structures, which seem to lose their coherence. It should be stressed that this decrease of $\overline{u'^2}$ downstream of the overshoot occurs in sections where the external level of $\overline{p'^2}$ increases. Therefore it seems that energy is transferred from the turbulent motion to the acoustic fluctuations in the external flow. Also, it may be noted that the 'turbulent' Mach number $\langle u' \rangle / a$ is about 0.27 at the maximum, which would indicate that compressibility effects can occur (Sarkar *et al.* 1989; Zeman 1990). Thus, the asymptotic mixing layer would be obtained through a region producing significant vertical velocity fluctuations contributing to a widening of the layer and creating pressure fluctuations in the external flows. As speculated in §4.1 a candidate for explaining this trend could be the pairing of the eddies. It would yet be necessary to explain why the pairing occurs in a rather well-defined part of the flow. The coupling due to pressure waves travelling in the subsonic flow could participate in such a phenomenon. However, this needs to be explored systematically in future experimental work, initiated in Dupont *et al.* (1993). It should also kept in mind that an increase in the three-dimensionality of the large eddies, as previously reported by Clemens & Mungal (1990) and Samimy, Reeder & Elliot (1992), may occur and will have to be checked by measurements.

An attempt was also made to use the turbulent diffusion model to estimate the convection velocity U_c. This velocity can be extracted from relation (3) as

$$U_c = \frac{(\overline{-u'v'})_{max}/(\Delta U)^2}{(\mathrm{d}\delta/\mathrm{d}x)(K/\Delta U)}. \tag{9}$$

Knowing K, $\mathrm{d}\delta/\mathrm{d}x$ and $(\overline{-u'v'})_{max}/(\Delta U)^2$ for each mixing layer it becomes possible to obtain an estimate of U_c from (9).

This was done in Barre, Dupont & Dussauge (1992*b*) for all the studied mixing layers using the value $K = 0.17$. The values of U_c given by this method are scattered because of the uncertainties in $\overline{-u'v'}$ and $\mathrm{d}\delta/\mathrm{d}x$: these quantities are known with an error of the order of 10% and so it is difficult to recommend the use of relation (9) as an accurate method for determining U_c'. However, it is interesting to note that an overall agreement was found with the available direct measurements. Three classes of flows were found: layers where U_c is close to the isentropic estimation, and cases where U_c is close to either U_1 or U_2. The few experiments where the confinement is not large are in the first class. This is the case for our experiment, for which preliminary direct determination of U_c from two-point hot-wire measurements (Barre *et al.* 1992*b*) confirmed this result. It was argued in Si-Ameur *et al.* (1992) and in Barre (1993) that confinement could be the cause of non-isentropic values of U_c, for convective Mach numbers in the range 0.5 to 1. This sort of results suggests the following picture: if the present diffusion scheme holds and if the value of K is not affected by compressibility up to $M_c = 1$ (and equal to the value given by the present experiment), the normalized diffusion time is the same for all the flows. For fully developed layers, the scatter

observed in the spreading rate (see figure 19) would be due to non-isentropic convection velocities, and may be related to the confinement of the flows.

A last point which requires some comment is the relation between the speed of sound sources and the convection velocity of the large structures. A simple and perhaps naïve guess could consist in assuming that the flow is formed of nearly two-dimensional structures with attached Mach waves. Then, if the latter are the main sound sources, the source speed would be essentially the convective velocity. As noticed previously, U_s in the developed part of the layer is practically the low-speed stream velocity, $U_s \approx 100\ \mathrm{m\ s^{-1}}$, while the isentropic convective velocity is $U_c = 311\ \mathrm{m\ s^{-1}}$. An interpretation of this result may be proposed by considering linear stability theory. Blumen, Drazin & Billings (1975) have shown that for $M_c > 1$ there can exist unstable modes having supersonic phase speeds with respect to one external flow and subsonic with respect to another one. A perturbation with phase speed close to the lower velocity can radiate noise into the other external flow. In the present case ($M_c = 0.62$) such convection velocities are found, but at a Mach number lower than those of the theoretical prediction, so that the main noise sources have a phase speed very different from the convection velocity.

5. Conclusions

The experiment presented in this work describes the evolution of mean and turbulent fields from boundary layers to a turbulent mixing layer at a convective Mach number of $M_c = 0.62$. The turbulent Mach number based on the r.m.s. velocity is in the range 0.27–0.3, such that characteristics of compressible turbulence can be found. One of the goals of this study was to produce a flow with low external levels of turbulence and well-defined initial conditions. The experimental method was elaborated with particular care in order to confirm experimental knowledge of the structure of turbulence in supersonic mixing layers. At the last measurements stations, the mixing layer was close to self-similarity. It was also verified that the properties of the developed mixing layer do not depend critically on the initial conditions. A simple turbulent diffusion model was developed as a guide for the interpretation of the results. In this model, compressibility mainly affects eddy viscosity and convection velocity; a diffusion constant K, which is proportional to the ratio of the turbulent friction and the spread rate, has to be determined from experiments as a function of density ratio and Mach number. The first conclusion from this experimental determination is that K does not depend on convective Mach number for $M_c < 0.62$ and also probably for $M_c < 1$. This supports the idea that the turbulent diffusion time is the relevant parameter of the problem. A consequence is that turbulent friction decreases with the Mach number proportionally to the spreading rate, and the diffusion model seems to be suitable for representing the effect of the Mach number on such layers.

The influence of compressibility on $\overline{u'^2}$ is not so clear. The present measurements suggest that the ratio $\overline{u'^2}/-\overline{u'v'}$ may be larger than in low-speed layers, and accordingly the anisotropy of the Reynolds stress tensor may vary. For larger M_c, existing data show contradictory trends, but a modification in the anisotropy is a likely guess at high convective Mach numbers. Well-controlled experiments are needed to address this point. In the present experiment, the developed state of the mixing layer is achieved through an overshoot in the level of $\overline{u'^2}$ accompanied by strong radiation of acoustic fluctuations in the external flows.

Some aspects of the influence of high speeds on the turbulence structure in supersonic mixing layers have been evaluated and clarified. The conclusions confirm

that turbulent diffusion in free shear flows depends mainly on large-scale structures and that compressibility effects on statistical quantities like Reynolds stresses can be observed for $M_c \geqslant 0.6$, but some new experiments are required to check the influence of Mach number on turbulence anisotropy, and on its space–time properties, like the three-dimensionality of the large-scale structures and their convection velocity.

Part of this work was supported by a grant of the G.D.R DRET-CNRS No. 917 'Hypersonique'. The encouragement of O. Leuchter at a preliminary stage of this work and the discussions with H. Fernholz are gratefully acknowledged. The authors are also very grateful to H. Fiedler who provided some original subsonic data used in this work to clarify the interpretation. Special thanks go also to D. R. Smith for his comments on the manuscript.

REFERENCES

ARZOUMANIAN, E. & DEBIÈVE, J. F. 1989 Un processus programmé pour les mesures par anémométrie à fil chaud en écoulement supersonique. *European Telemetry and Test Conf., Marseille, France, June 1989.*

BARRE, S. 1993 Estimate of convective velocity in a supersonic turbulent mixing layer. *AIAA J.* (to appear).

BARRE, S., DUPONT, P. & DUSSAUGE, J. P. 1992*a* Hot wire measurements in turbulent transonic flows. *Eur. J. Mech.* B *Fluids* **11**, 439–454.

BARRE, S., DUPONT, P. & DUSSAUGE, J. P. 1992*b* Convection velocity of large scale structures in a supersonic mixing layer. *IUTAM Symp. Eddy Structure Identification in Free Turbulent Shear Flows, Poitiers, France, October 1992.*

BELL, J. H. & MEHTA, R. D. 1990 Development of a two-stream mixing layer with tripped and untripped boundary layers. *AIAA J.* **28**, 2034–2042.

BIRCH, S. F. & EGGERS, J. M. 1973 Free turbulent shear flows. *NASA Rep.* SP-321.

BLUMEN, W., DRAZIN, P. G. & BILLINGS, D. F. 1975 Shear layer instability of an inviscid compressible fluid. Part 2. *J. Fluid Mech.* **71**, 305–316.

BOGDANOFF, D. W. 1983 Compressibility effects in turbulent shear layers. *AIAA J.* **21**, 926–927.

BONNET, J. P. & DEBISSCHOP, J. R. 1993 Experimental studies of the turbulent structure of supersonic mixing layers. *AIAA Paper* 93-0217.

BRADSHAW, P. 1966 The effect of initial conditions on the development of a free shear layer. *J. Fluid Mech.* **26**, 225–236.

BRADSHAW, P. & FERRISS, D. H. 1971 Calculation of boundary layer development using the turbulent energy equation: compressible flow on adiabatic walls. *J. Fluid Mech.* **46**, 83–110.

BROWN, G. L. & ROSHKO, A. 1974 On density effects and large structures in turbulent mixing layers. *J. Fluid Mech.* **64**, 775–781.

CHINZEI, N., MASUYA, G., KOMURO, T., MURAKAMI, A. & KUDOU, K. 1986 Spreading of two stream supersonic turbulent mixing layer. *Phys. Fluids* **29**, 1345–1347.

CLEMENS, N. T. & MUNGAL, M. G. 1990 Two- and three-dimensional effects in the supersonic mixing layer. *AIAA Paper* 90-1978.

DEBISSCHOP, J. R. 1993 Comportement de la turbulence en couches de mélange supersoniques. Thèse de Doctorat de l'Université de Poitiers.

DIMOTAKIS, P. E. 1986 Two-dimensional shear-layer entrainment. *AIAA J.* **24**, 1791–1796.

DIMOTAKIS, P. E. 1991 Turbulent free shear layer mixing and combustion. *Prog. Astronaut. Aeronaut.* **137**, 265–340.

DJERIDANE, T., AMIELH, M., ANSELMET, F. & FULACHIER, L. 1993 Experimental investigation of the near-field region of variable density turbulent jets. *5th Intl Symp. on Refined Flow Modelling and Turbulence Measurements, Paris, France, September 7–10, 1993* (submitted).

DUPONT, P. & DEBIÈVE, J. F. 1989 A measurement method of temperature and velocity fluctuations from transonic to supersonic regimes. *European Telemetry and Test Conf., Marseille, France, June, 1989.*

DUPONT, P., BARRE, S., DELBOULBE, E. & DUSSAUGE, J. P. 1993 Space-time properties of supersonic turbulent mixing-layers. *Symp. on Transitional and Turbulent Compressible Flows, 1993 ASME Fluids Engineering Conf., Washington, DC, June 20–23, 1993* (to be presented).

DUTTON, J. C., BURR, R. F., GOEBEL, S. G. & MESSERSMITH, N. L. 1990 Compressibility and mixing in turbulent free shear layer. *12th Symp. on Turbulence, Missouri-Rolla, Sept. 1990.*

DZIOMA, B. & FIEDLER, H. E. 1985 Effect of initial conditions on two-dimensional free shear layer. *J. Fluid Mech.* **152**, 419–442.

ELLIOTT, G. S. & SAMIMY, M. 1990 Compressibility effects in free shear layers. *Phys. Fluids* A **2**, 1231–1240.

FERNHOLZ, H. H. 1971 Ein halbempirisches Gesetz für die Wandreibung in kompressiblen turbulenten Grenzschichten bei isothermer und adiabater Wand. *Z. Angew. Math. Mech.* **51**, 146–147.

FIEDLER, H. E., LUMMER, M. & NOTTMEYER, K. 1990 The plane mixing layer between parallel streams of different velocities and different densities. *Proc. MHD and Turbulence Conf., Jerusalem, 1990.* AIAA.

GAVIGLIO, J. 1987 Reynolds analogies and experimental study of heat transfer in the supersonic boundary layer. *Intl J. Heat Mass Transfer* **30**, 911–926.

HALL, J. L. 1991 An experimental investigation of structure, mixing and combustion in compressible turbulent shear layers. PhD thesis, California Institute of Technology.

HINZE, J. O. 1959 *Turbulence.* McGraw Hill.

HORSTMAN, C. C. & ROSE, W. C. 1977 Hot wire anemometry in transonic flows. *AIAA J.* **15**, 395–401.

IKAWA, H. 1973 Turbulent mixing layer experiment in supersonic flow. PhD thesis, California Institute of Technology.

IKAWA, H. & KUBOTA, T. 1975 Investigation of supersonic turbulent mixing layer with zero pressure gradient. *AIAA J.* **13**, 566–572.

KISTLER, A. L. 1959 Fluctuation measurements in a supersonic turbulent boundary layer. *Phys. Fluids* **2**, 290–296.

KLEBANOFF, P. S. 1955 Characteristics of turbulence in a boundary layer with zero pressure gradient. *NACA Rep.* 1247.

KLINE, S. J., CANTWELL, B. J. & LILLEY, G. M. 1980 *Proc. 1980 Conf. on Complex Turbulent Flows,* Vol. I, pp. 364–366. Stanford University.

KOVASZNAY, L. S. G. 1953 Turbulence in supersonic flows. *J. Aero. Sci.* **20**, 657–682.

LAU, J. C. 1981 Effects of exit Mach number and temperature on mean flow and turbulence characteristics in round jets. *J. Fluid Mech.* **105**, 193–218.

LAU, J. C., MORRIS, P. J. & FISHER, M. J. 1979 Measurements in subsonic and supersonic free jets using a laser velocimeter. *J. Fluid Mech.* **93**, 1–27.

LAUFER, J. 1961 Aerodynamic noise in supersonic wind tunnels. *J. Aerospace Sci.* **28**, 685–692.

LIEPMANN, H. & LAUFER, J. 1947 Investigation of free turbulent mixing. *NACA TN* 1257.

LIEPMANN, H. & ROSHKO, A. 1962 *Eléments de la Dynamique des Gaz.* Gauthier-Villars.

MCINTYRE, S. S. & SETTLES, G. S. 1991 Optical experiments on axisymmetric compressible turbulent mixing layers. *AIAA Paper* 91-0623.

MILES, J. W. 1958 On the disturbed motion of a plane vortex sheet. *J. Fluid Mech.* **4**, 538–552.

MORKOVIN, M. V. 1956 Fluctuations and hot-wire aneomometry in compressible flows. *AGARD* 24.

MORKOVIN, M. V. 1962 Effects of compressibility on turbulent flows. *Colloque sur la Mécanique de la Turbulence, Marseille, France, Aout 1961.*

NORMAN, M. L. & WINKLER, A. 1985 Supersonic jets. *Los Alamos Science, Spring/Summer 1985.*

NOTTMEYER, K. 1990 Experimentelle Untersuchung der Ausbildung und Turbulenzstruktur von turbulenten Scherschichten zwischen Gasströmen unterschiedlicher Geschwindigkeit und Dichte. PhD thesis, Technische Universität Berlin, Hermann-Föttinger-Institut für Thermo-und Fluiddynamik.

OERTEL, H. 1979 Mach wave radiation of hot supersonic jets investigated by means of the shock tube and new optical techniques. *Proc. 12th Intl Symp. of Shocks Tubes and Waves,* Jerusalem, pp. 266–275.

PAI, S. I. 1954 On the stability of a vortex sheet in an inviscid compressible fluid. *J. Aero Sci.* **21**, 325–328.

PANCHAPAKESAN, N. R. & LUMLEY, J. L. 1993*a* Turbulence measurements in axisymmetric jets of air and helium. Part 1. Air jet. *J. Fluid Mech.* **246**, 197–223.

PANCHAPAKESAN, N. R. & LUMLEY, J. L. 1993*b* Turbulence measurements in axisymmetric jets of air and helium. Part 1. Helium jet. *J. Fluid Mech.* **246**, 225–247.

PAPAMOSCHOU, D. 1986 Experimental investigation of heterogeneous compressible shear layers. *PhD thesis, California Institute of Technology.*

PAPAMOSCHOU, D. 1989 Structure of the compressible turbulent shear layer. *AIAA Paper* 89-0126.

PAPAMOSCHOU, D. & ROSHKO, A. 1988 The compressible turbulent shear layer: an experimental study. *J. Fluid Mech.* **197**, 453–477.

PETRIE, H. L., SAMIMY, M. & ADDY, A. L. 1986 Compressible separated flows. *AIAA J.* **24**, 1971–1978.

QUINE, C. 1990 Etude expérimentale et numérique de couche de mélange turbulentes supersoniques et isobares. Thèse de doctorat, Université d'Aix-Marseille II.

SAMIMY, M. & ELLIOTT, G. S. 1990 Effects of compressibility on the characteristics of free shear layers. *AIAA J.* **28**, 439–445.

SAMIMY, M., PETRIE, H. L. & ADDY, A. L. 1986 A study of compressible turbulent reattaching free shear layer. *AIAA J.* **24**, 261–267.

SAMIMY, M., REEDER, M. F. & ELLIOTT, G. S. 1992 Compressibility effects on large structures in free shear flows. *Phys. Fluids* A **4**, 1251–1258.

SANDHAM, N. D. & REYNOLDS, W. C. 1989 Growth of oblique waves in the mixing layer at high Mach number. *Seventh Symp. on Turbulent Shear Flows, Stanford University, August 1989.*

SARKAR, S., ERLEBACHER, G., HUSSAINI, M. Y. & KREISS, H. O. 1991 The analysis and modelling of dilatational terms in compressible turbulence. *J. Fluid Mech.* **227**, 473–493.

SCHLICHTING, H. 1964 *Layer Theory*, 6th edn. McGraw-Hill.

SI-AMEUR, M., GATHMANN, R., CHOLLET, J. P. & MATHEY, F. 1992 Turbulence dans les écoulements supersoniques libres ou confinés, couches de mélange et jets. *Colloque sur les Écoulements Hypersoniques, Garchy, France, 5–7 October 1992.*

SIRIEIX, M. & SOLIGNAC, J. L. 1968 Contribution à l'étude expérimentale de la couche de mélange turbulent isobare d'un écoulement supersonique. *Symp. on Separated Flows, AGARD Conf., Proc.* vol. 4, pp. 241–270.

SMITS, A. J. & DUSSAUGE, J. P. 1989 Hot wire aneomometry in supersonic flow. *AGARD* 315.

SMITS, A. J., SPINA, E. S., ALVING, A. E., SMITH, R. W., FERNANDO, E. M. & DONOVAN, J. F. 1989 A comparison of the turbulence structure of subsonic and supersonic boundary layers. *Phys. Fluids* A **1**, 1865–1875.

WAGNER, R. D. 1973 Mean flow and turbulence measurements in a Mach 5 free shear layer. *NASA TN* D7366.

WYGNANSKI, I. & FIEDLER, H. 1970 The two-dimensional mixing region. *J. Fluid Mech.* **41**, 327–361.

ZEMAN, O. 1990 Dilatation dissipation: the concept and application in modeling compressible mixing layers. *Phys. Fluids*, A **2**, 178–188.

ZEMAN, O. 1992 Similarity in supersonic mixing layers. *AIAA J.* **30**, 1277–1283.